BNL-105873-2014-TECH

EP&S No. 158;BNL-105873-2014-IR

Estimated induced activity using danger parameters

A. J. Stevens

August 2001

Collider Accelerator Department

Brookhaven National Laboratory

U.S. Department of Energy

USDOE Office of Science (SC)

DISCLAIMER

For Internal Distribution Only

Experimental Support and Facilities Division
Collider-Accelerator Department
BROOKHAVEN NATIONAL LABORATORY
Upton, New York 11973

ES&F Division Technical Note # 158

ESTIMATING INDUCED ACTIVITY USING **'DANGER PARAMETERS'**

A. J. Stevens

August 2, 2001

Estimating Induced Activity Using 'Danger Parameters'

A.J. Stevens, 08/02/2001

I. Introduction

This note discusses the use of Barbier's 'Danger Parameters'[1] as a tool to estimate induced radioactivity. Most of the discussion is not concerned with practical applications, although one reasonably complicated example is given, but with the systematic errors associated with how well the Danger Parameters are known.

The gamma ray danger parameter DP is given by Eqn. (7.1) in Ref. [1]. In slightly re-written form it is:

$$(1) \qquad DP = 3.6\times10^{6}\,\frac{N_0}{A_T}\sum_i\sum_p \frac{\varepsilon_{i,p}(e_p)\,\rho_T}{f_p(e_p)\,\mu_{p,T}(e_p)}\,\sigma_{i,T}\,[1-\exp(-t_r/\tau_i)]\exp(-t_c/\tau_i)$$

mrad/hr per particle/cm^2-sec

In this expression:

N_0 is Avagadro's number,
A_T is the atomic weight of the Target(T),
$\sigma_{i,T}$ is the cross section for the production of radionuclide i (from target material T),
ρ_T is the density,
$\varepsilon_{i,p}(e_p)$ is the probability of nuclide i emitting photon p with energy e_p,
$\mu_{p,T}$ is the (energy dependent) attenuation coefficient for photon p,
f_p is an (energy dependent) factor for converting photon flux to dose equivalent,
τ_i is the mean life of isotope i,
t_r is the irradiation time, and
t_c is the cooling time.

To first approximation, the induced activity at a point P from a body uniformly activated by a hadron flux ϕ and which defines solid angle $\delta\omega$ at a point P is given by:

$$(2) \qquad Ac(P) = DP\times\phi\times\frac{d\omega}{4\pi}$$

This is illustrated in Fig. 1. Both σ and ϕ depend on the energy and type of the irradiating hadron which is not explicitly displayed.

Equation (1) needs to be 'corrected' for a number of effects,[2] the most important of which is photon 'build-up,' – the scattering of photons which modifies the simplistic use of the (linear) absorption coefficient in Eqn. (1). An approximation for the build-up factor (for this case of uniform activation) is given in Fig. I.40 of Barbier; 'typically' it increases DP by a factor of 2.

Curves of DP for various materials (and at several irradiating energies – in particular at 50 MeV and 500 MeV) are given in Appendix B of Barbier. This author has rather casually used these curves, together with a variety of approximations needed to evaluate 'real world' geometries, in making induced activity estimates. This note describes an attempt to reconstruct DP from Eqn (1), instead of using the curves. Initially, this author believed that all the information needed to do so was contained in Ref. [1]. However, a more careful reading of Barbier leads to ambiguities which, in turn, have something to say about uncertainties which underlie such 'casual use' of the curves for DP as found in Ref. [1].

In the next section, the varied uncertainties are discussed. In Section III, an evaluation of DP from Eqn. (1) is discussed (for $A_T < Cu^{65}$) and some comparisons to Barbier's graphs are made. Section IV illustrates an example application. Finally, Appendix 1 shows Excel graphs of DP constructed as described Section III for various materials that may be of some use.

II. Uncertainties in Evaluating Danger Parameters

Two of the parameters in Eqn. (1) have been taken directly from expressions given in Ref. [1] without critical evaluation. The attenuation coefficient is taken from the expression given in Eqn. (6.7) of Ref. [1] to be:

$$\frac{m}{r}(E, A_T, Z_T) = 1.8\times10^{-5}\frac{Z_T^{1.05}}{A_T}(10E)^{-3} + 0.1267\frac{Z_T}{A_T}(E)^{-0.45} + 3.52\times10^{-4}\frac{Z_T^2}{A_T}[3.11\ln(3.92E) - 8.07]$$

Where μ/ρ is in $cm^2 g^{-1}$ and E is in MeV.[3] Likewise, the flux to dose equivalent is taken from Eqns. (5.1) and (5.2) of Ref. [1] to be:

$$f = \begin{cases} 1.45\times10^{13} E^2\ cm^{-2} rad^{-1} & for\ E < 0.053\,MeV \\ 2.10\times10^{9}\ E^{-1}\ cm^{-2} rad^{-1} & for\ 0.053 < E < 5\,MeV \end{cases}$$

In the discussion of the Danger Parameter in Barbier, it is stated that spallation cross-sections are taken from the formula of Rudstam, which is given in Chapter 2 of Ref. [1] in several equations and graphs. This is, a priori, the 'ingredient' that one expects to be the most uncertain. Several seemingly careful caveats to the use of the Rudstam cross sections, however, turn uncertainty into ambiguity. On page 103 of Ref. [1] one finds the following sentence. "It should be noted that the [Rudstam] cross-section formula cannot be expected to hold right up to the target, and no product nearer to the target than two mass units has been considered…" On page 107, the following appears. "…as the [Rudstam] formula is not expected to be good below A = 20." And finally, on page 186, in discussing the (relatively high) energy regions where cross-sections are approximately constant with energy, one finds "It is in this region that Rudstam's formula can be considered to apply rather well." However, in Appendix B, where the graphs of DP are given, one finds a graph for a C^{12} target at 50 MeV in which the radionuclide

C^{11} is manifestly present, a situation which violates all three of the cautions about using the Rudstam formula!!

Before returning to the subject of uncertainty in the spallation cross-sections, another potential uncertainty will be considered (and dispensed with). This uncertainty relates to the emitted photons. In evaluating the Danger Parameters, Barbier ignores all radionuclides with photons having half lives less than 5 minutes, and, consistent with this, shows DP for cooling times greater than .01 days (~ 14 minutes). The nuclides considered are listed in Appendix A of Ref. [1]. In this listing is included the *sum of photon emission probabilities*. Now, in fact, this is the only sensible thing to put in such a listing, since the number of photons varies greatly by nuclide. The only point here is that one cannot reconstruct DP values without recourse to references other than Barbier. In particular, the emission probability of 'each' photon is needed since the quantity being summed in Eqn (1) depends on photon energy. One 'gamma ray catalog,' conveniently in the BNL Library, is Erdtmann and Soyka.[4] (The time required to obtain photon information from the literature grows exponentially with atomic mass because of the increasing number of radionuclides. As this author has a limited amount of time to devote to this study, **only target materials with A_T below 65 (Cu^{65}) have been examined.**)

There are, however, seemingly problems with the nuclides listed in Appendix A of Barbier. One problem is the absence of nuclides that are expected to be present. Examples include $_{19}K^{45}$ and $_{21}Sc^{49}$, both gamma emitters with half lives well over 5 minutes. Whether they were included in the evaluation of the danger parameters and simply omitted from Appendix A by oversight is not known. Other problems become apparent when comparing Barbier to Erdtmann. In most cases, the sum of emission probabilities agree (within 20% or so), but in some cases there are large differences. An example here is that the long-lived isomer of $_{17}Cl^{34}$ has a summed emission probability of 1.03 in Barbier and 2.84 in Erdtmann. However, to shorten a long story, two estimates of values for DP from Eqn. (1) for a wide variety of materials were made treating photons differently. In the first variant, only the nuclides listed in Barbier's Appendix A were considered. Although the photon energies were taken from Ref. [4] (Erdtmann), the emission probabilities were re-normalized to the total given by Barbier. In the second variant, the information in the Erdtmann reference alone was used. All radionuclides with half lives greater than 1 minute, including those with half-lives greater than 5 minutes not listed in Appendix A of Barbier for unknown reasons, were included. Considering nuclides with half-lives between 1 and 5 minutes is not really important and was done simply to get some rough estimate of activity at shorter access times. **No significant difference was observed in the values of the Danger Parameters constructed using these two 'photon sets.'**[5] In what is given in the remainder of this document, the 'Erdtmann photons' were used.

As a prelude to returning to the subject of the dominant uncertainty of the spallation cross-sections, some aspects of how the danger parameters will be used must be considered. In many, if not most instances, the activating flux are neutrons with an exponentially decreasing energy spectrum. In the past this author as made the simplifying assumption that the activating flux is hadrons above 20 MeV, a reasonably conservative 'typical' threshold energy for spallation. However, reaction thresholds vary widely, and the cross-section energy dependence near 'threshold' is strong. In this author's opinion, Barbier chose '50 MeV' as essentially a euphemism for "average energy somewhat above reaction threshold" and '500 MeV' as a

euphemism for "average energy where the cross-sections have become essentially constant with energy."[6]

The mystery of where the input for Barbier's danger parameter curve for C^{12} at 50 MeV is seemingly solved by the discovery of the representation of measured data in Chapter 4. This author's interpretation of most of that data is given in Table 1 below.

Table 1. Cross-Section Data Read from Graphs in Chapter 4 of Ref. [1] See text.

Tgt	(Nuclide, E)	(Value,Particle)	Used	Comment
C^{12}	(C^{11}, 50)	(22,n)	22	plateau by 50 mev; p very large (85)
C^{12}	(Be^{7},50)	(16,p)	16	
C^{12}	(C^{11},500)	(25.5,p-n)	25.5	average of n,p
C^{12}	(Be^{7},500)	(11,p)	11	
O^{16}	(O^{15},50)	(80,p)	80	50 mev about peak
O^{16}	(N^{13},50)	(5,p)	15	ave. in 20-30 mev range
O^{16}	(C^{11},50)	(13,p)	12	ave. in 30-60 mev range
O^{16}	(Be^{7},50)	(1.7,p)	2.2	ave. in 50-60 mev range
O^{16}	(O^{15},500)	(40,p)	40	
O^{16}	(N^{13},500)	(5,p)	5	
O^{16}	(C^{11},500)	(11,p)	11	
O^{16}	(Be^{7},500)	(6,p)	6	
Al^{27}	(Na^{24},50)	(26,n)	80	ave. in 10-20 mev range; peak about 120 mb at 13 mev.
Al^{27}	(Na^{22},50)	(28,p)	17	ave. in 30-50 mev range
Al^{27}	(F^{18},50)	(3,p)	2	ave. in 40-60 mev range
Al^{27}	(Na^{24},500)	(18,p-n)	18	average of n,p
Al^{27}	(Na^{22},500)	(14,p)	14	
Al^{27}	(F^{18},500)	(8,p)	8	
Al^{27}	(Be^{7},500)	(3,p)	3	rising at 500!
Fe	(Fe^{52},50)	(3.8,p)	3.2	ave. in 30-50 mev range
Fe	(Mn^{54},50)	(55,p)	40	ave. in 30-50 mev range
Fe	(Mn^{52},50)	(12,p)	18	ave. in 30-50 mev range
Fe	(Cr^{51},50)	(52,p)	30	ave. in 30-50 mev range
Fe	(V^{48},50)	(4,p)	8	ave. in 30-40 mev range
Cu	(Cu^{61},50)	(55,p)	60	ave. in 30-50 mev range
Cu	(Ni^{57},50)	(1,p)	1	ave. in 40-60 mev range
Cu	(Co^{60},50)	(14,p)	12	ave. in 30-60 mev range
Cu	(Co^{57},50)	(54,p)	20	ave. in 30-50 mev range
Cu	(Co^{56},50)	(1,p) (at 52 MeV)	3	ave. in 50-60 mev range

The first column of Table 1 gives the target material. The second column gives the measured nuclide species at either 50 or 500 MeV. The third column gives the production cross-section (in mb.) for this nuclide and the incident particle type (p or n for proton or neutron). The fourth column gives **the cross-section value this author has decided to use as a part of the definition of the '50 MeV' danger parameters.** Consider two examples. The measured cross-

section for the production of Na^{24} by 50 MeV neutrons on Al is about 26 mb. However, the cross-section peaks at about 120 mb. at 13 MeV, and is about 80 mb when averaged over the 10 MeV – 20 MeV interval. (See the 'Comments' column of Table 1.) Since the irradiating flux *will be approximated by the 'generic' sum of hadrons above 20 MeV*, the 80 mb. number will be used to compensate for the fact that a substantial fraction of the low energy flux will be neglected. **Since the purpose of using danger parameters is associated with safety, this 'massaging' of the cross-section is intended to be somewhat conservative**.[7] As a second example, consider the cross-section for the production of Cr^{51} from Fe (natural) by 50 MeV protons. The cross-section at 50 MeV is actually about 52 mb. However, this value is near the peak, and the cross section averaged in the 30 to 50 MeV interval is about 30 mb., and 30 MeV is about the threshold. Again, counting nucleons above 20 MeV is conservative, or would be conservative in the approximation of n,p symmetry, which brings up another uncertainty.

It seems fairly clear from the text of Barbier that neutrons are not distinguished from protons. In the 'high energy' regime (i.e., what is called here 500 MeV) this is not a bad approximation. However, near threshold, the asymmetries can be very large. Note from the 'Comment' column of Table 1 that the production of C^{11} by protons on C^{12} is 4 times larger than by neutrons (since, of course, a deuteron is 'easy' to make). However, in the overwhelming number of practical situations, neutrons completely dominate the near-threshold flux. For this reason, this author has chosen to use the neutron cross-sections data where it exists. Another aspect of n,p asymmetry is mentioned in the next section.

III An Evaluation of Danger Parameters and Comparison to Barbier's Graphs

It is clear, then, that substantial uncertainties exist related to nuclide cross-sections, even in the very limited cases where data exists. In order to get some feeling as to the magnitude of this uncertainty, two evaluations of DP from Eqn. (1) have been made, varying (to some extent) the radionuclide cross-sections. Besides the data in Table 1 and the Rudstam formula, one other source of information is available to this author, namely the cross-sections given by the MCNPX code.[8] However, to the best of this author's knowledge,[9] the cross-sections in MCNPX stem from a 'high-energy' model in the LAHET code, and are – like the Rudstam formula – not expected to be correct near threshold. It is at least mildly interesting to compare what MCNPX and the Rudstam formula give at 50 MeV (neither distinguishes between n and p) with the 'massaged' cross-sections given in Table 1. This is shown in Table 2 below. If one blindly averages the ratios of 'model' to data for the 23 entries in Table 2 having the massaged data > 5 mb., then the MCNPX/Data ratio is .83 and the Rudstam/Data ratio is 1.17. There are 7 MCNPX entries (of 23) more than a factor of 3 lower than the data and 9 similar Rudstam entries. If the comparison is limited to the area where both models are supposed to be reasonable – at 500 MeV and ignoring the A_T –1 isotopes for Rudstam – such 'global statistics' do not change significantly. For a specific target, however, it is clear that differences between the data and one or the other of the model cross-sections sets might lead to significant differences in the estimated danger parameter.

Table 2. "Massaged" Cross-Section Data Vs. MCNPX and Rudstam

Tgt	(Nuclide, E)	s ('Data' – mb.)	MCNPX s *	Rudstam s **
C^{12}	(C^{11}, 50)	22	19	(64)
C^{12}	(Be^{7},50)	16	11	1.2
C^{12}	(C^{11},500)	25.5	34	(7.2)
C^{12}	(Be^{7},500)	11	10	3.6
O^{16}	(O^{15},50)	80	15.5	(56)
O^{16}	(N^{13},50)	15	1.7	8.4
O^{16}	(C^{11},50)	12	10	1.2
O^{16}	(Be^{7},50)	2.2	2.6	<.005
O^{16}	(O^{15},500)	40	37	(6.1)
O^{16}	(N^{13},500)	5	4.2	4.7
O^{16}	(C^{11},500)	11	9	3.5
O^{16}	(Be^{7},500)	6	<.005	1.8
Al^{27}	(Na^{24},50)	80	7.3	43
Al^{27}	(Na^{22},50)	17	8.6	5.0
Al^{27}	(F^{18},50)	2	0.4	<.005
Al^{27}	(Na^{24},500)	18	7	23
Al^{27}	(Na^{22},500)	14	17	14
Al^{27}	(F^{18},500)	8	9.5	9.2
Al^{27}	(Be^{7},500)	3.2	<.005	<.005
Fe	(Fe^{52},50)	3	<.005	<.005
Fe	(Mn^{54},50)	40	164	306
Fe	(Mn^{52},50)	18	3.2	18
Fe	(Cr^{51},50)	30	8.5	21
Fe	(V^{48},50)	8	<.005	.2
Cu	(Cu^{61},50)	60	38	84
Cu	(Ni^{57},50)	1	<.005	<.005
Cu	(Co^{60},50)	12	28	29
Cu	(Co^{57},50)	20	8.8	2.5
Cu	(Co^{56},50)	3	1.4	<.005

* The MCNPX were derived from short runs and have about 10% statistical error.
** Parentheses around the Rudstam values marks the A_T-1 nuclides.

With this comparison between data and models in mind, a comparison which does not greatly distinguish one model vs. the other, two sets of cross-sections were formed Both data sets have the following in common:

- The massaged 'data' given in Table 1 (or 2) is used.

- For nuclides with atomic weight of A_T or A_T –1, the MCNPX cross-sections were used.

The remaining nuclides (if any) were chosen for Set 1 to be the average of the Rudstam and MCNPX cross-sections and for Set 2 the MCNPX cross-sections at 50 MeV and the Rudstam cross-sections at 500 MeV.

A word is necessary regarding the nuclides with mass A_T (charge exchange). In adding the charge exchange cross sections from MCNPX neutrons must, in principle, be distinguished from protons. At 50 MeV it has been assumed that only neutrons are present, so that the cross-section for $p,{}^{Z}A_T \rightarrow n,{}^{Z+1}A_T$ is ignored. At 500 Mev, a 50-50 mixture of n and p are assumed, so the cross-sections are simply averaged.

Danger Parameters were calculated for '50' and 500 MeV for irradiation times of 1, 7, 30, and 360 days for the following materials: C, SiO_2, $CaCO_3$, Al, Fe, Ni, and Cu. (SiO_2 is Barbier's approximation of concrete and $CaCO_3$ is marble). The results (Set 1, Set 2, and Barbier's graph) are shown in Figures 2 through 15 for the 30 day irradiation period.

In general, the agreement is quite good, almost always within a factor of 2. The relatively large "discrepancy" for C at 50 MeV is apparently simply because Barbier has chosen to use the much larger proton data as discussed above.[10] The worst real discrepancy is between the Barbier graphs and the Set 2 calculation for SiO2 at 50 MeV. This is due entirely to the Si component, and is due to a very small Na^{24} estimate by MCNPX. Note from Table 2 that the same problem would exist for an Al target in the absence of data. Most other cases of relatively large differences (Al at 50 MeV or Ni at 500) are due to adding significant A_T and/or $A_T - 1$ cross-sections from MCNPX to both estimates made here.

On one hand, the good agreement between the estimates here and the graphs of Barbier might be dismissed as inevitable since so much – namely the data and Rudstam cross-sections – are in common. On the other hand, potentially significant differences do exist. The data has been interpreted differently, an equal mixture (for Set 1) of different 'model' cross-sections has been added, nuclides have been added (the MCNPX A_T and $A_T - 1$ cross-sections), and a different 'photon set' has been used. Given these differences, the factor of 2 agreement (except for the well-understood Carbon target) validates the expectation that the danger parameters are good to within a factor of 2 or 3. It should be noted however that this conclusion depends on the existence of the measured data. The accuracy of the danger parameters for the higher mass targets given in Barbier is more speculative. Excel charts of the 'Set 1' Danger Parameters are shown in Appendix 1.

V. An Example Application

In this section an application will be made to region of the MECO primary target.[11] The *approximation* of the geometry of that region is shown in Fig. 16. In this cylindrical approximation an 8 GeV proton beam is incident on a (barely visible) 0.5 cm radius, 16 cm. long tungsten target located at Z = 70 cm. Most of the shield material shown is copper. However, the coil support and cryo. wall are Fe and the end plate is Al. The goal of the exercise is to use Eqn. (2) in Section I above estimate the induced activity at the points indicated in Fig. 16 (which are all 1 ft. away from the nearest surface) given an irradiation of 4×10^{13} protons/sec on target for 30 days.

There are many approximations required to apply danger parameters to a "real world" geometry. As an initial example, consider the fact that the hadron flux in the material falls

rapidly as a function of distance from the target. This violates the "uniform irradiation" assumption of the danger parameter. It is clear that the most relevant point of flux evaluation is near the outside of the object – since the attenuation length of photons is significantly shorter than that of the hadron flux, but the question is how near?

To answer this question in an approximate manner, a cylinder of Fe was considered. The fall-off of hadrons with energy greater than 20 MeV is given by something like

$$\frac{\exp(-R / \boldsymbol{l}_H)}{R^2}$$

where R is the transverse radius and $\boldsymbol{l}_H$ is 21 cm.[12] Getting the attenuation length for the photons is more uncertain. In creating the photon data file as a part of the danger parameter calculations, it became clear that a somewhat conservative estimate for the average photon energy would be 1 MeV.[13] To use the attenuation length from the expression given at the beginning of Section II above for the linear attenuation coefficient would not be correct, because there is no accounting for build-up (photon scattering), and the question being asked here concerns the probability of photons emerging from points within the object where their production probability is higher due to the higher hadron flux. Without belaboring the point further, a photon shielding code (Microshield) was used to obtain an estimate of an effective attenuation length in Fe for a 1 MeV photon of about 3 cm.[14] Calculating the flux at this depth from the surface compensates for the fact that the irradiation is not constant.

The remaining approximations are best explained by considering the highly schematic "side view" of the geometry shown in Fig. 17. In this view the outer cryo. wall surface (see Fig. 16) subtends the angle shown at point P. Let this surface, within this angle, be considered a source of photons for which the irradiating flux has been calculated. Since it is not infinitely thick, the danger parameter for Fe can be applied here *but it must be de-rated.* It should be reasonably clear that the de-rating factor should be $1 - \exp(-t/\lambda)$ where t is the thickness of the wall and λ the effective attenuation length discussed above.

Now the inner cylinder in Fig. 17 is also a source of photons. This is supposed to correspond to the coil and coil-support regions shown more accurately in Fig. 16. Again, photons are emitted towards P from a surface subtending a smaller angle as shown. In this case, the thickness is (effectively) infinite, but the outer cylinder attenuates the photons by $\exp(-t/\lambda)$. For the particular case chosen, t being 2 cm. and λ 3cm, both factors related to the cryo. wall are about 0.5. An additional approximation is needed for the inner cylinder source because the 2 cm. thick coil is (approximately) Cu whereas the 5 cm. coil support is Fe. For the purpose of this estimate, the simple average of the two danger parameters will be used.

Consider one of the points of evaluation shown outside the cryo. wall in Fig. 16. Any of these points "sees" the two cylindrical surfaces discussed above as sources of emitted photons. A straight forward computer program segments each surface into smallish areas dA and approximates the solid angle at the point P by dA_T/R^2 where the subscript T denotes the perpendicular distance from P to the center of dA.[15] The approximation of Eqn. (2) to estimate the activity at one of the points outside the cryo. wall in Fig. 16 is then:

$$(3) \qquad Ac(P) = \frac{B}{4\pi} \sum_{S} \sum_{Z} \sum_{j} f(x,y,z) \times DP_{corrected} \frac{dA_T}{R^2}$$

Where S indicates a sum over the two surfaces considered, Z and φ sums over the dimensions of each surface, and "corrected" indicates the approximations discussed above. B is the build-up factor mentioned in the very beginning of this note and evaluated as discussed in the next paragraph. One Point in Fig. 16 – clearly different from the rest – is shown 1 ft. downstream of the (aluminum) end plate. This point is the "hot spot," since it is at a small angle with respect to the beam. In this case, three surfaces are considered: the aluminum end plate, the downstream Cu shield block, and the beam pipe. Similar to the transverse case discussed above, the end plate and the beam pipe are de-rated because they are thin, and the Al shields (to some extent) photons coming from the downstream Cu block.[16]

As stated in the Introduction, the photon build-up factor for uniformly irradiated bodies is not contained in the danger parameters. Barbier's Figure I.40 has this correction to be about a factor of 2, but states that no correction need be made for very thin or small cross-section bodies. This factor was independently evaluated using the Microshield code, again for a 1 MeV photon. For very thick Fe, the build up factor was found to be 1.89. For the two nominally 'thin" bodies, the 2 cm-thick cryo. wall and the 5 cm. Al endplate, this code obtained build-up factors of 1.35 and 1.41 respectively.

The last approximation that will be mentioned is the low energy vs. high energy (i.e., 50 MeV vs. 500 MeV danger parameters) division. The flux was estimated using the MCNPX program, and the hadrons between 20 and 100 MeV were 'called' 50 MeV.

The results for the transverse points shown in Fig. 16 are shown in Fig. 18. The results for the "hot spot," is shown in Table 3 below.

Table 3. Activity at 'Hot Spot" for 30 days Irradiation at 4×10^{13}p/sec on Target.

Activity (rad/hr)	**Cooling Time**
72.0	1 hr.
25.8	1 day
2.52	10 days

VI. Conclusions

An estimate of the activity at these same points in the same structure had previously been made by this author by using the Danger Parameters as they appear in Barbier's graphs, together with the approximation that the 'typical photon' was 0.5 MeV instead of the 1 MeV assumed here. In that previous estimate, the highest point off to the side of the cryostat wall had been estimated to be 1.62 rad/hr. at 1 hr. cooling time instead of the 2.39 rad/hr. shown in Fig. 18, and the hot spot had been estimated to be 53.1 rad per hour at the 1 hr. cooling time rather than the 72.0 rad/hr. in Table 3. Much of the motivation for this tedious document was an attempt to

evaluate the systematic error associated with the previous estimate. The *differences* in the two estimates are: (1) a different set of danger parameters were used, (2) a different 'typical' photon energy was used to make approximations, (3) a different set of build-up factors was used, (4) different evaluations of the irradiating flux and of Eqn (3) were used. On the other hand, the similarities were (1) the data which plays a great role for the 50 MeV danger parameters was identical (although the interpretation was somewhat different, as discussed earlier), (2) the Rudstam formula is present in both danger parameter sets. (3) the same *code* (MCNPX) was used to evaluate the irradiating flux, and (4) the same *methodology* was used in applying the danger parameters to the physical situation. In this author's opinion, the differences are very small and to some extent no doubt reflect the conservative nature of the current estimate since, as mentioned in Section II above, the use of Danger Parameters is associated with radiation safety.

As was the case in considering two different cross-section sets for evaluation of the Danger Parameters in Section III, the 'repeat' of this example estimate validates the general claim is that use of Barbier's Danger Parameters should be good to a factor of 2 or 3 without considering errors in the evaluation of the irradiation flux. It is again pointed out that this conclusion is reached here only for targets with atomic mass of Cu and below.

References/Footnotes

1. M. Barbier, "Induced Radioactivity," John Wiley & Sons, Inc., New York, 1969.

2. Other effects not explicitly included by the use of Eqn. (1) are electrons and the effect of nuclear decay chains. The magnitude of the change in D due only to Compton electrons is shown in Fig. I.42 of Barbier to be ~ 20 – 30%.

3. The last term exists only when it is > 0.

4. G. Erdtmann and W. Soyka, "The Gamma Rays of the Radionuclides," Topical Presentations in Nuclear Chemistry, Vol. 7, Weinheim, New York, 1979.

5. Other minor differences existed in the two photon sets which are not discussed. In both variants the number of gamma rays has been restricted to 4, and the grouping of gammas for nuclides where more than 4 exist was done simply by eye from the data in Erdtmann. The differences in using these two photon sets was less than 10% in all the comparisons made.

6. Barbier also considers 2900 MeV for some materials. The difference between 2900 MeV and 500 MeV for the materials considered here (Cu and $CaCO_3$) is small. Even in the heavy targets considered by Barbier, the difference is only about a factor of 2.

7. Although it is difficult to claim that any particular situation is 'typical,' in a geometry where a 25 GeV beam is incident on an Fe target, then in the transverse direction after about 1 ft. of Fe, the neutron flux between 20 and 100 MeV is (according to Ref. [8] below) about 4 times larger

than the flux between 10 and 20 MeV. Counting only the neutrons between 20 and 100 MeV but assigning the lower energy cross-section is about a factor of 2 conservative, whereas making the same count, but assigning the 'more correct' cross-section of 26 mb. would underestimate the DP by about the same factor of 2.

8. L. S. Waters, Ed., "MCNPX USER'S MANUAL," LANL Report TPO-E83-UG-X-0001, (1999). See also H.G. Hughes, R.E. Prael, R.C. Little, "MCNPX – The LAHET/MCNP Code Merger," X-Division Research Note, 4/22/97. The version number of the code used in this note is 2.1.5.

9. A. Hanson, private communication.

10. Similarly for C at 500 MeV for short cooling times. Apparently Barbier has used the proton data for C^{11} whereas this author has averaged proton and neutron data.

11. Muon Electron COnversion experiment.

12. See, for example, K. Tesch and H. Dinter, "Estimation of Radiation Fields at High Energy Proton Accelerators," Rad. Prot. Dosimetry Vol. 15, No. 2 pp. 89-107 (1986).

13. In the past this author has used 0.5 MeV. While this energy is clearly the most probable energy (positron emitters give 2 0.51 MeV gammas), 1 MeV is clearly a better estimate of the average.

14. This result was obtained for a 1 MeV photon shielded by a spherical shell of Fe with radius 16 cm. from the MicroShield code of Grove Engineering. This code has a linear attenuation length of 2.24 cm. (for ρ = 7.8 g/cc) compared to the expression from Barbier given at the beginning of Section II which gives 2.17 cm.

15. The dot product between the vector from P to dA and the normal to the surface.

16. The 'effective' attenuation for a 1 MeV photon in Al was estimated to be 14.5 cm.

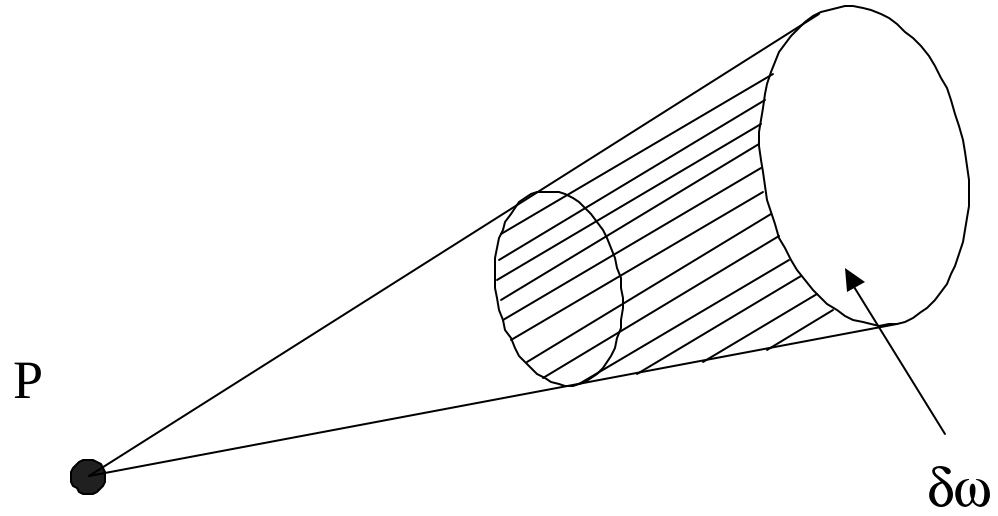

Fig. 1 Uniformly Activated Body Defining Solid Angle δω at Point P. The body is supposedly "Semi-infinite" in Depth.

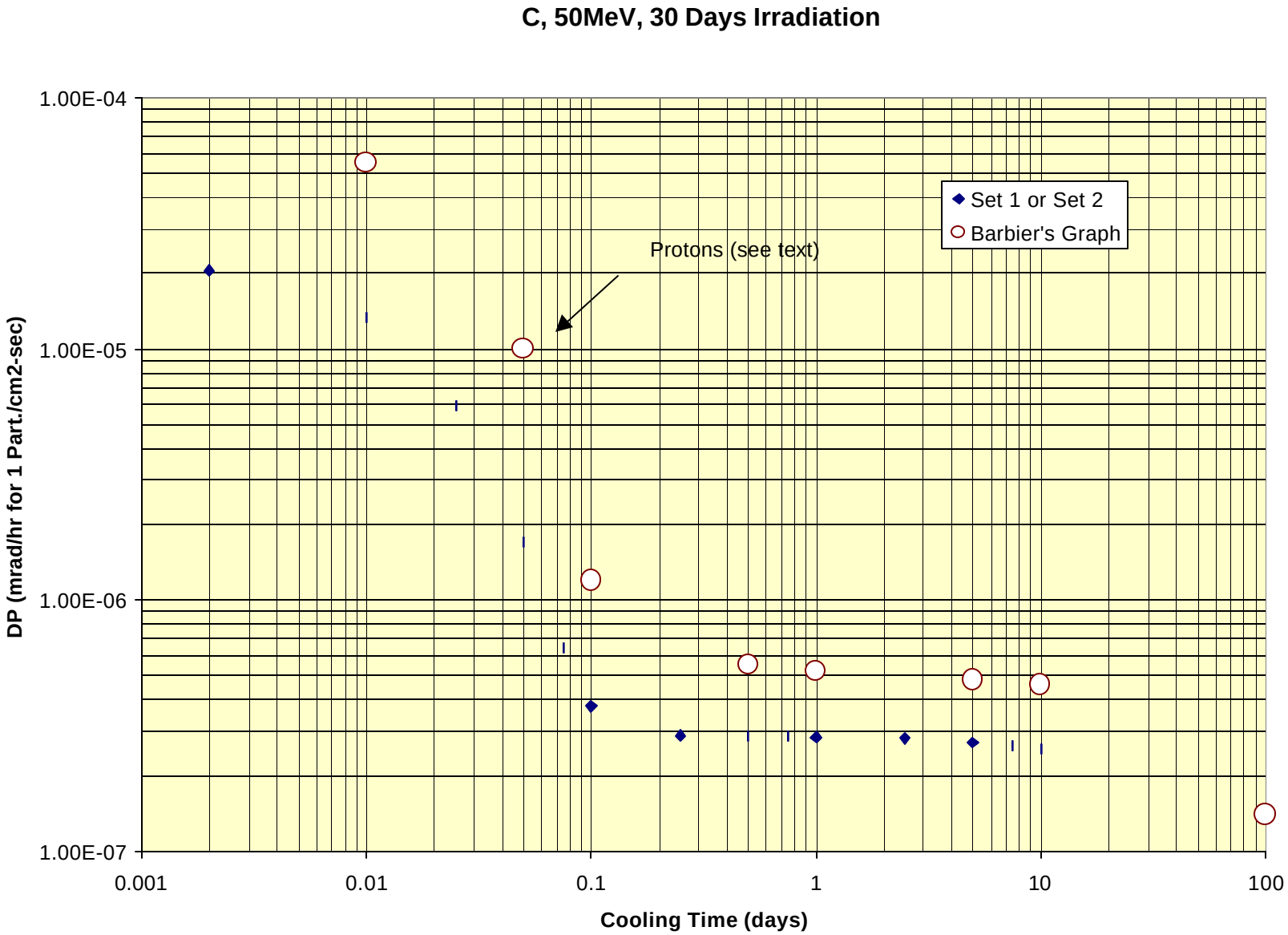

Fig. 2. Danger Parameter for C at 50 MeV and 30 Days Irradiation

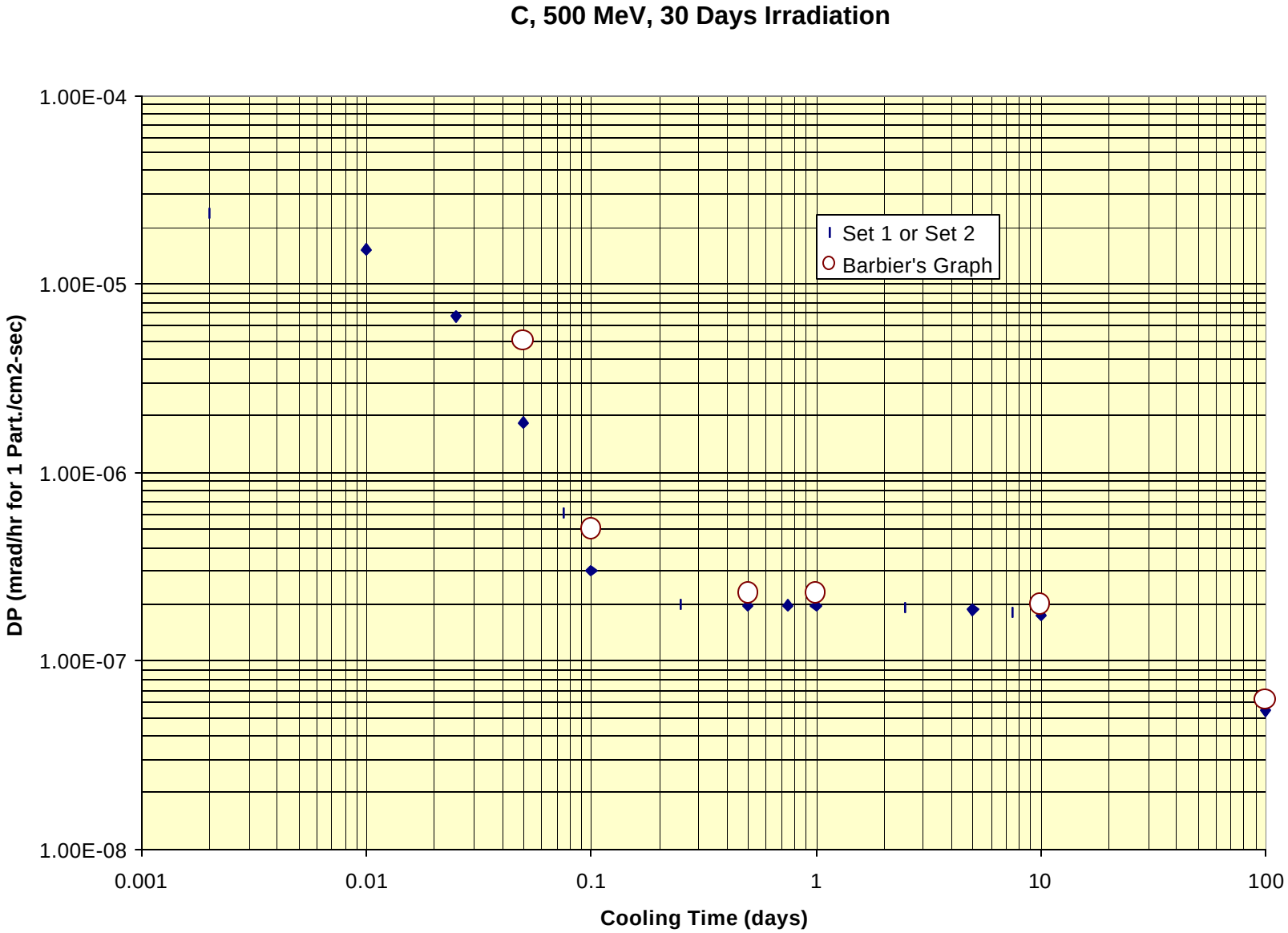

Fig. 3. Danger Parameter for C at 500 MeV and 30 Days Irradiation

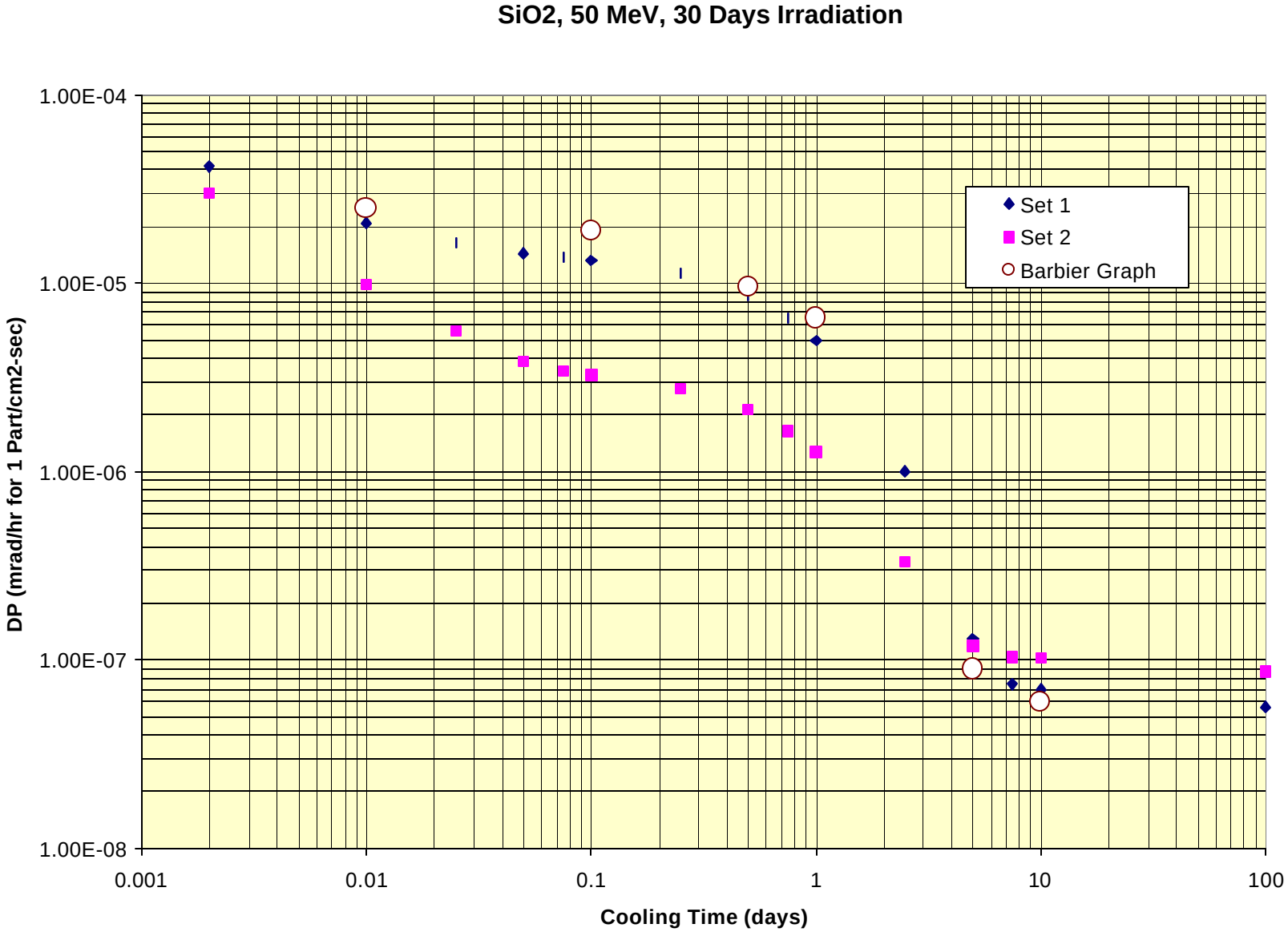

Fig. 4. Danger Parameter for SiO2 at 50 MeV and 30 Days Irradiation

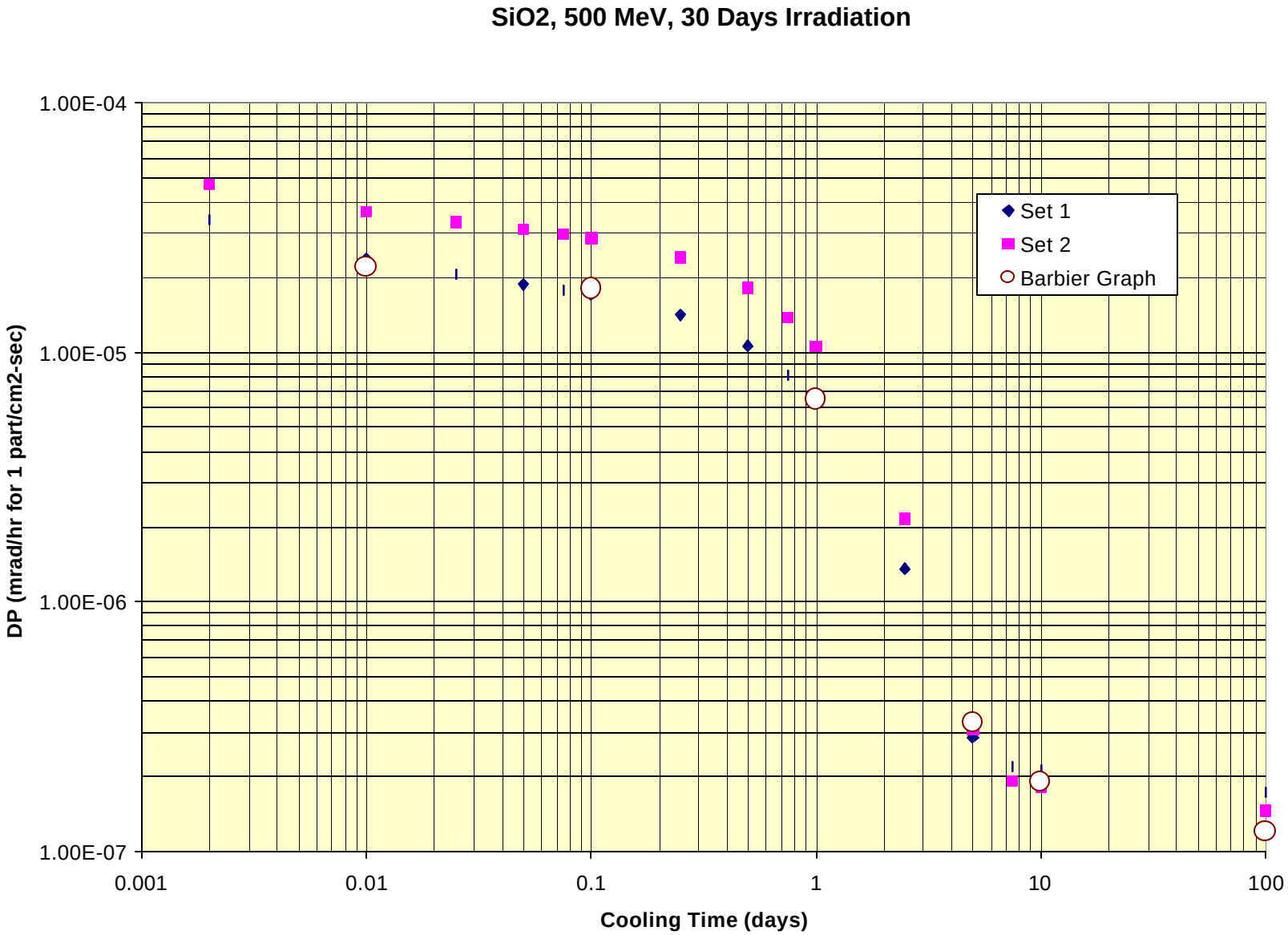

Fig. 5. Danger Parameter for SiO2 at 500 MeV and 30 Days Irradiation

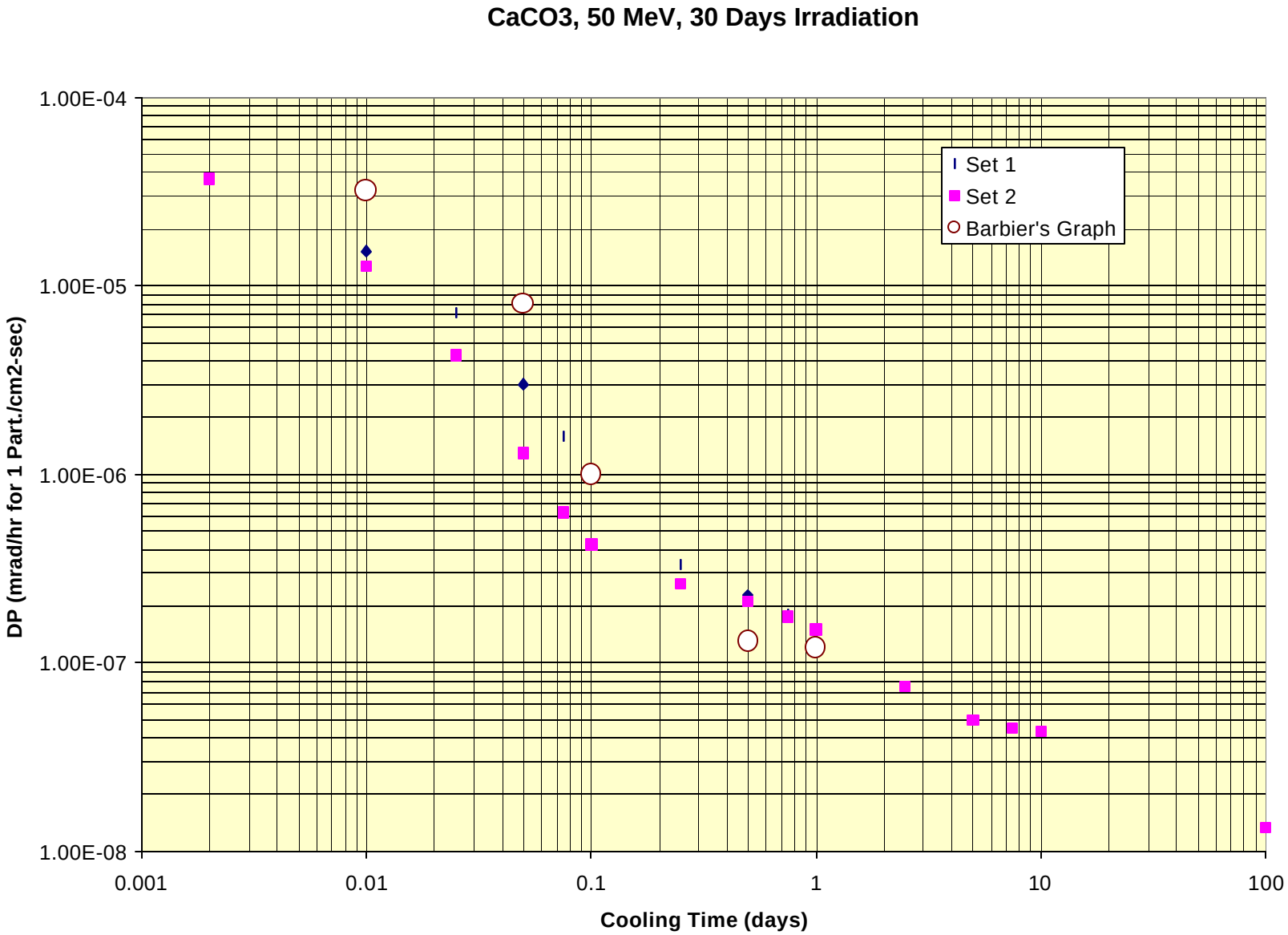

Fig. 6. Danger Parameter for $CaCO_3$ at 50 MeV and 30 Days Irradiation

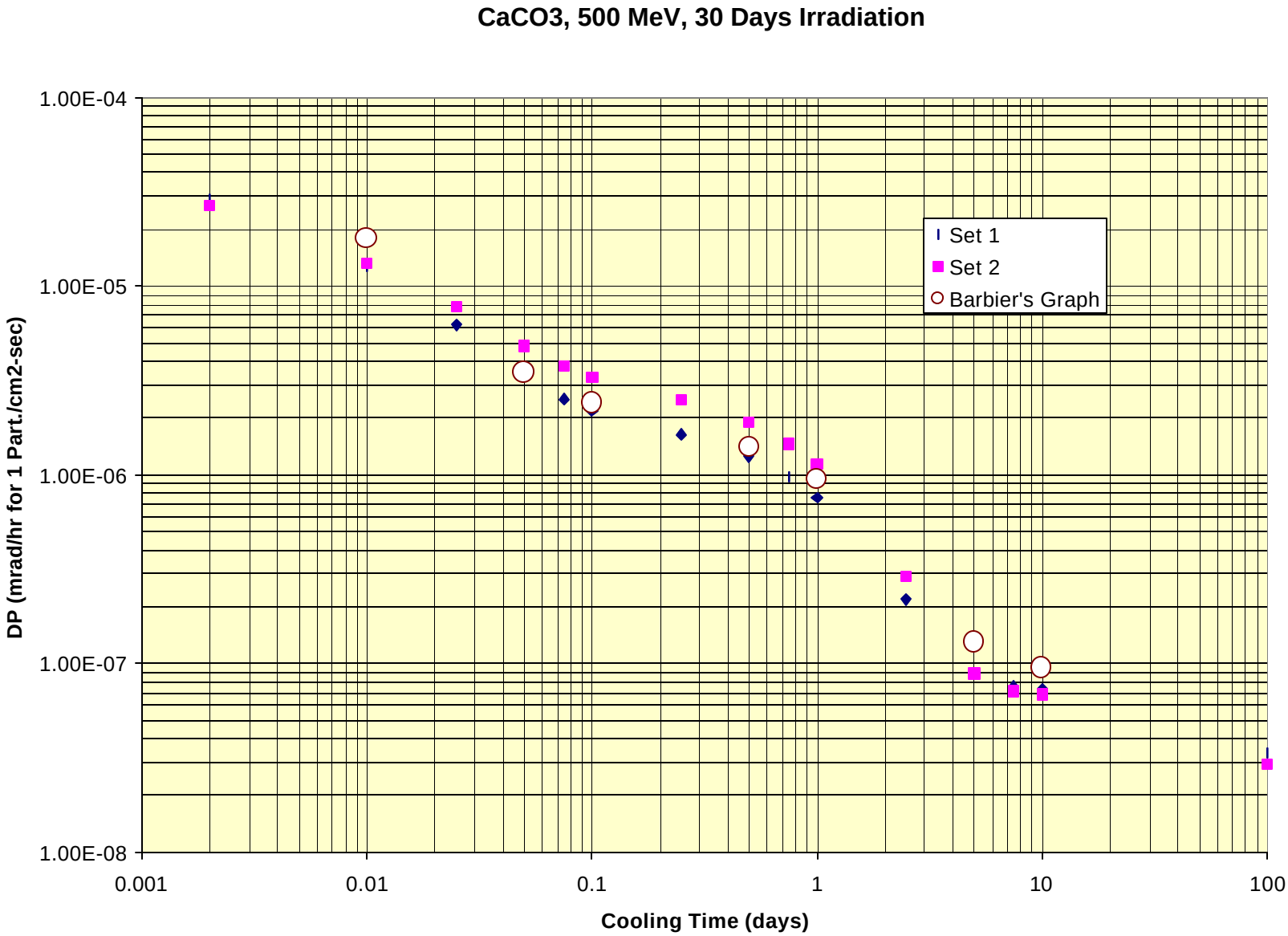

Fig. 7. Danger Parameter for $CaCO_3$ at 500 MeV and 30 Days Irradiation

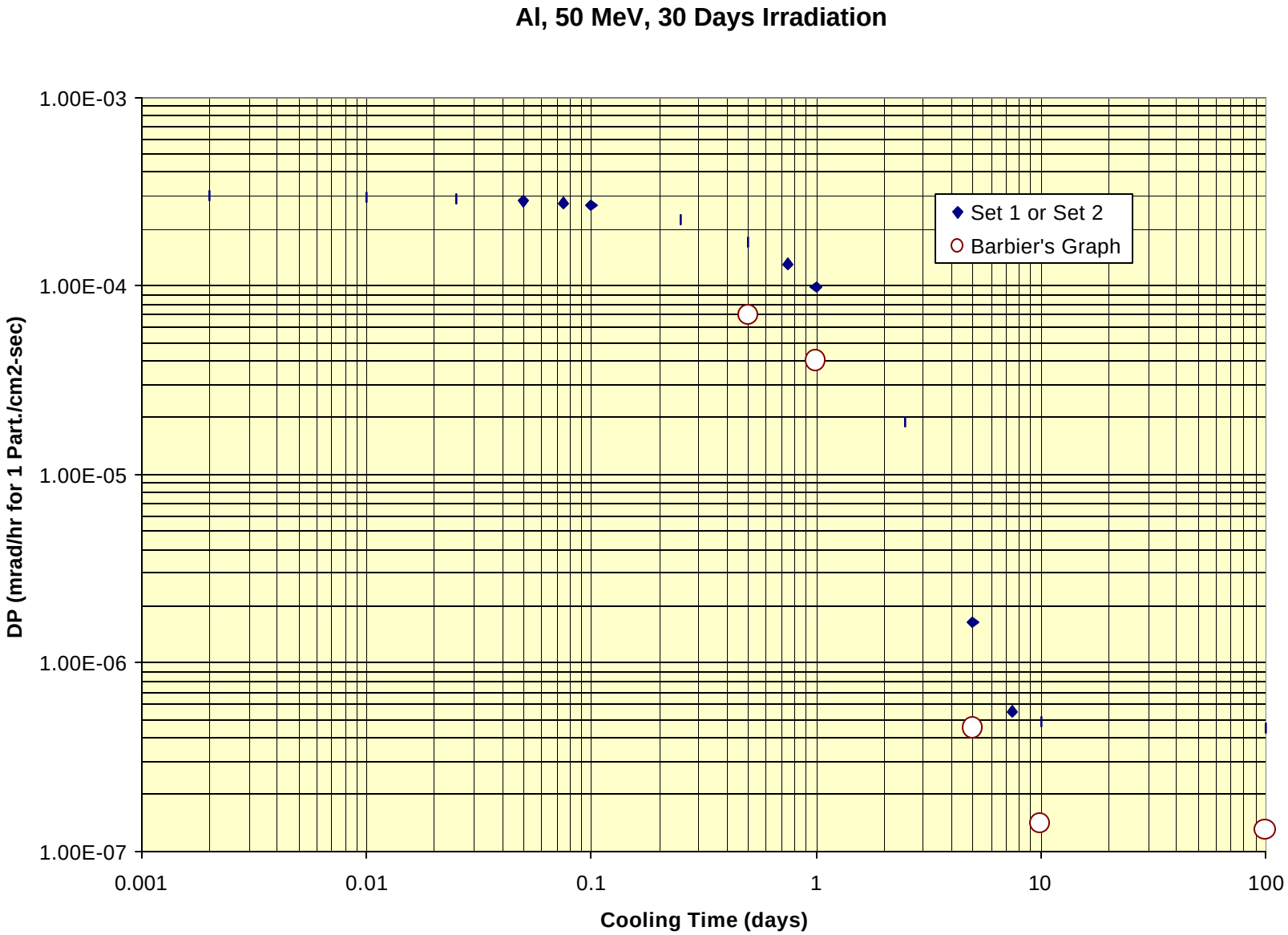

Fig. 8. Danger Parameter for Al at 50 MeV and 30 Days Irradiation

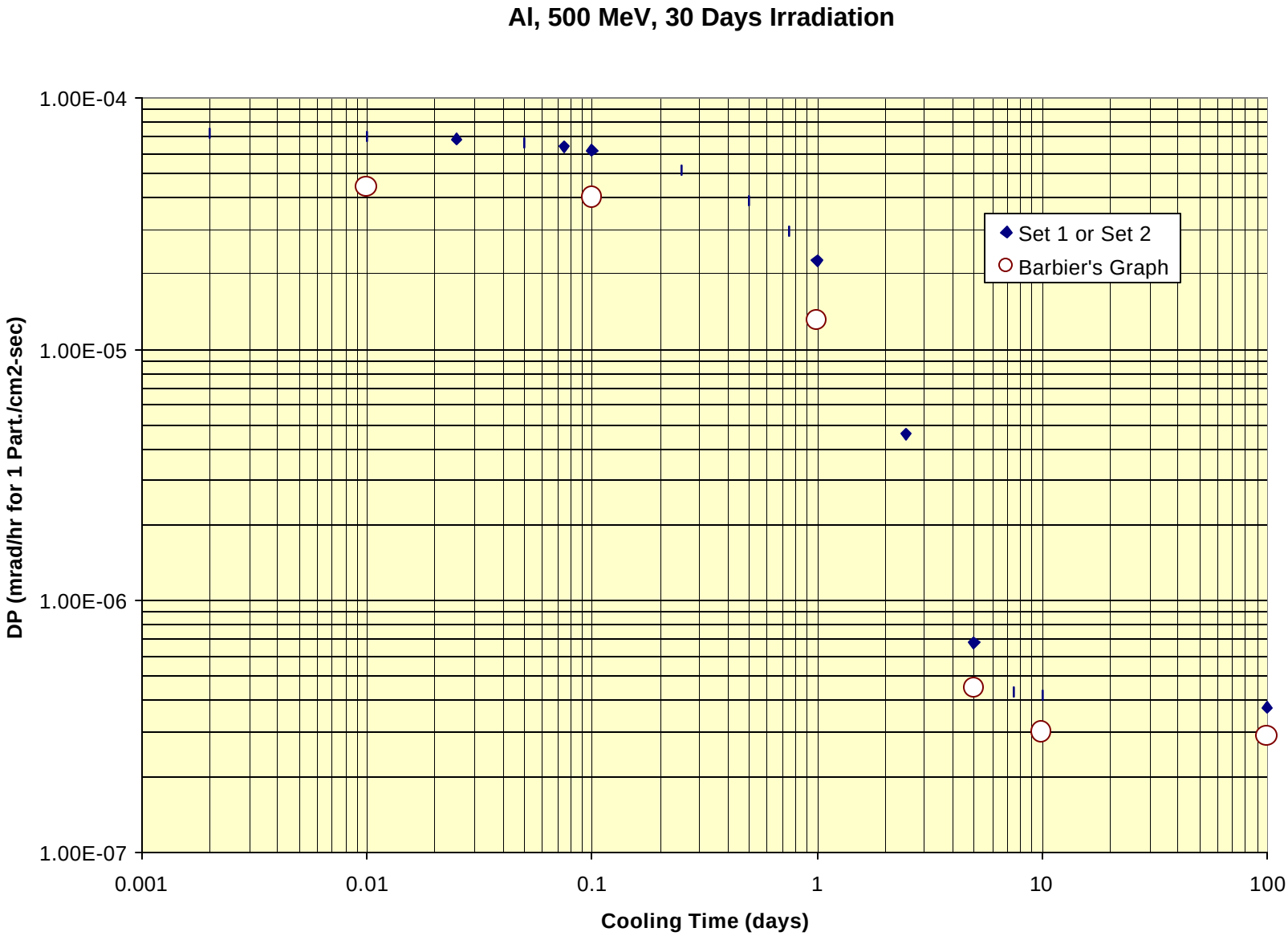

Fig. 9. Danger Parameter for Al at 500 MeV and 30 Days Irradiation

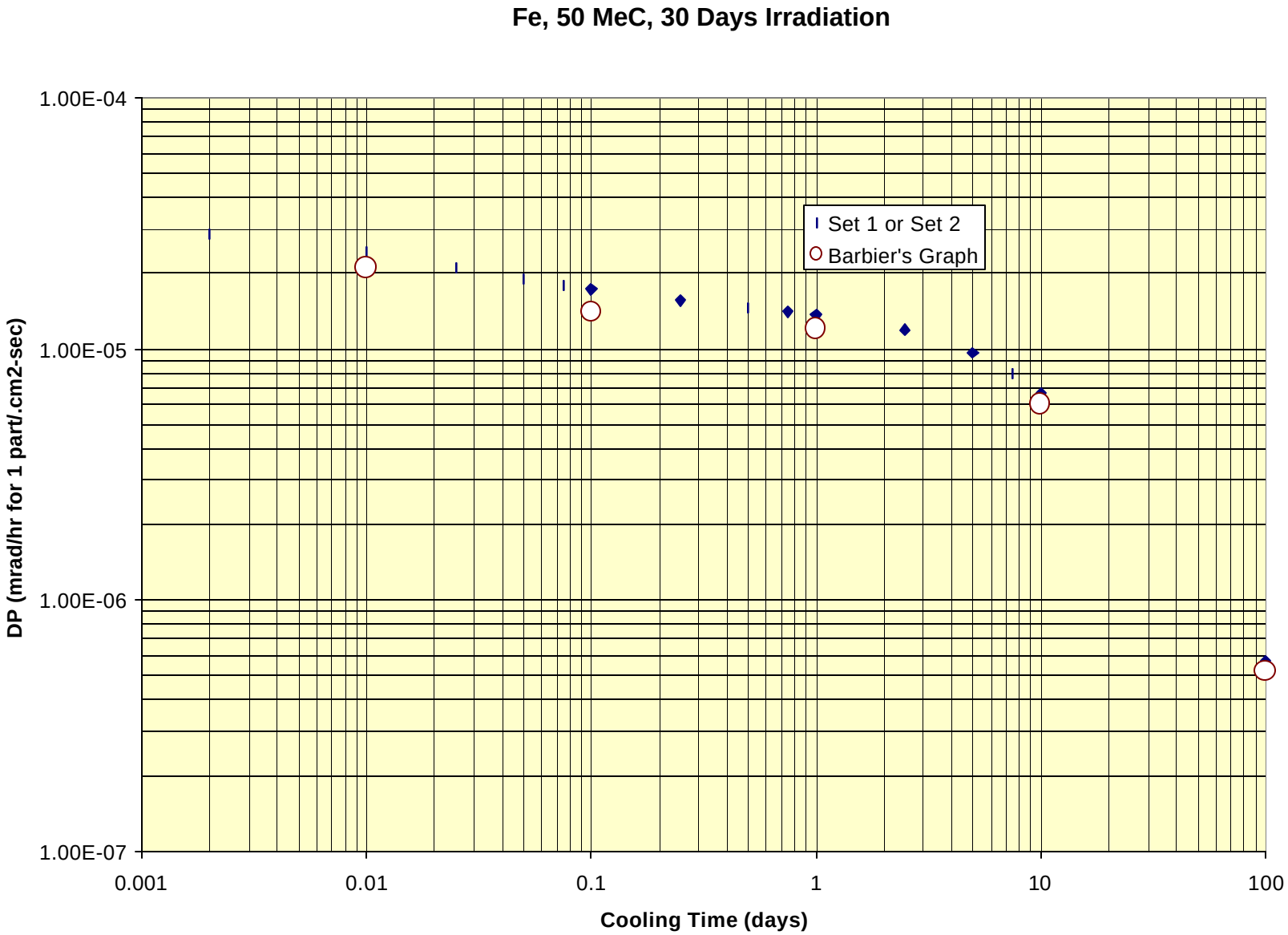

Fig. 10. Danger Parameter for Fe at 50 MeV and 30 Days Irradiation

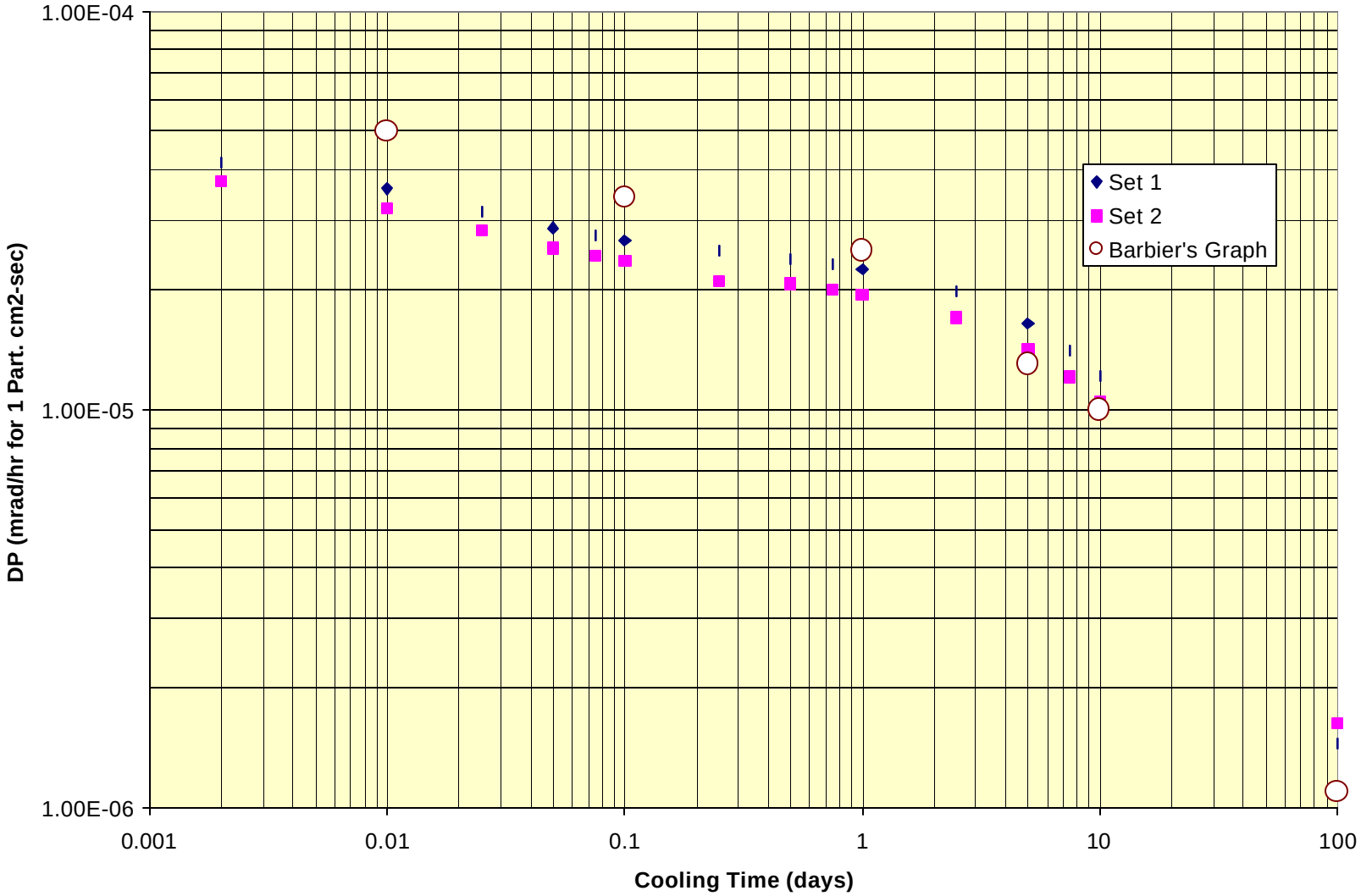

Fig. 11. Danger Parameter for Fe at 500 MeV and 30 Days Irradiation

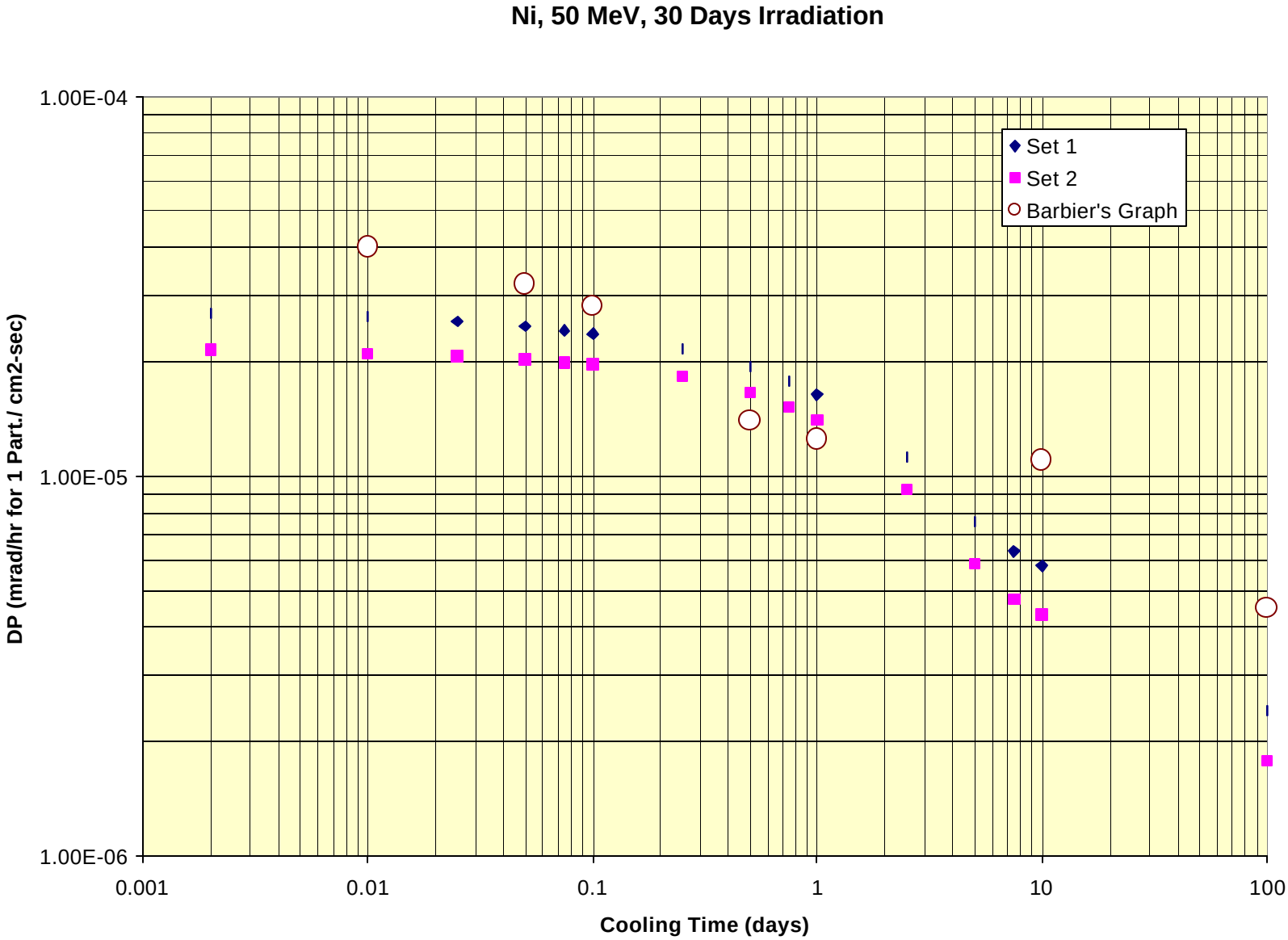

Fig. 12. Danger Parameter for Ni at 50 MeV and 30 Days Irradiation

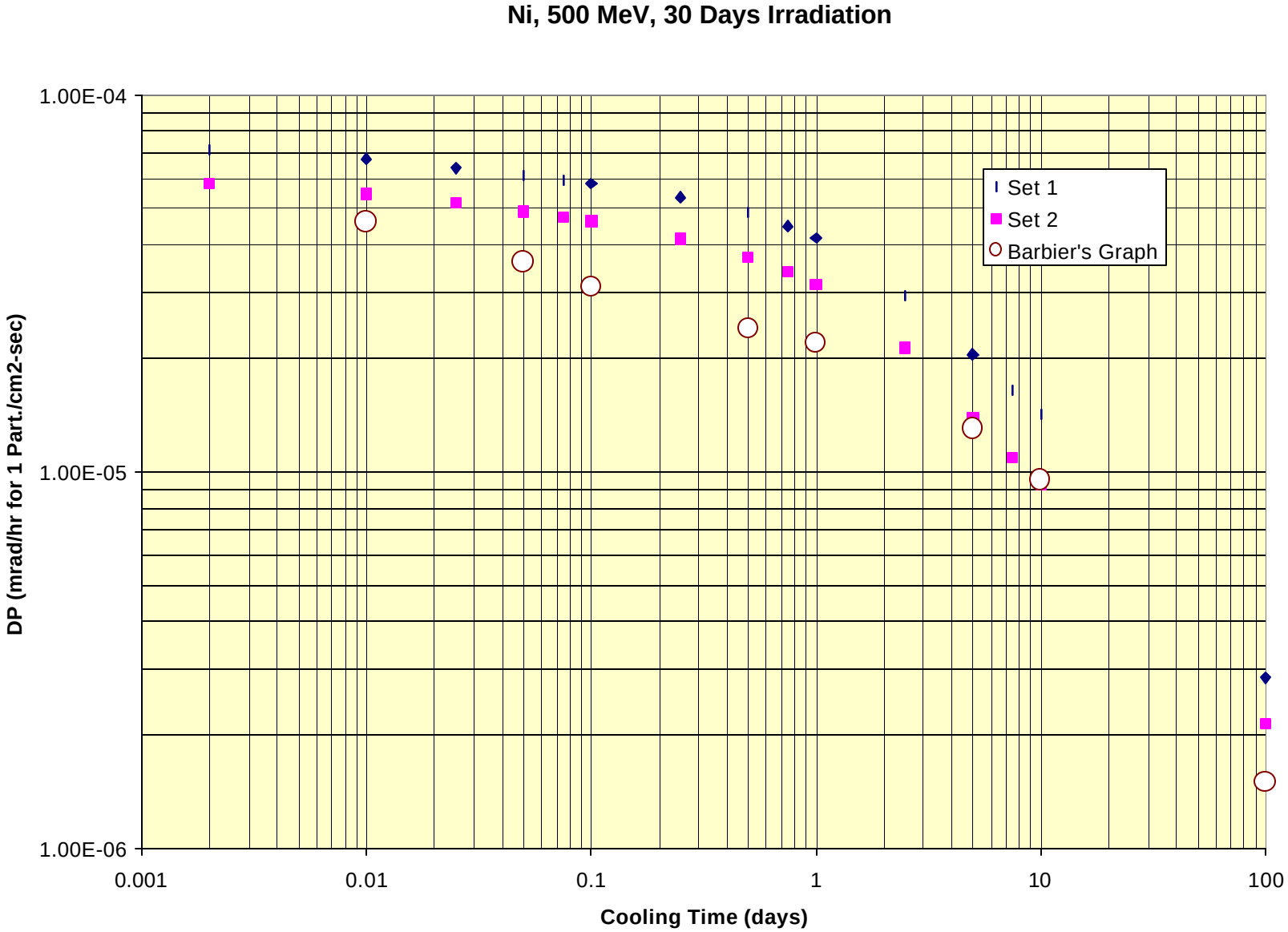

Fig. 13. Danger Parameter for Ni at 500 MeV and 30 Days Irradiation

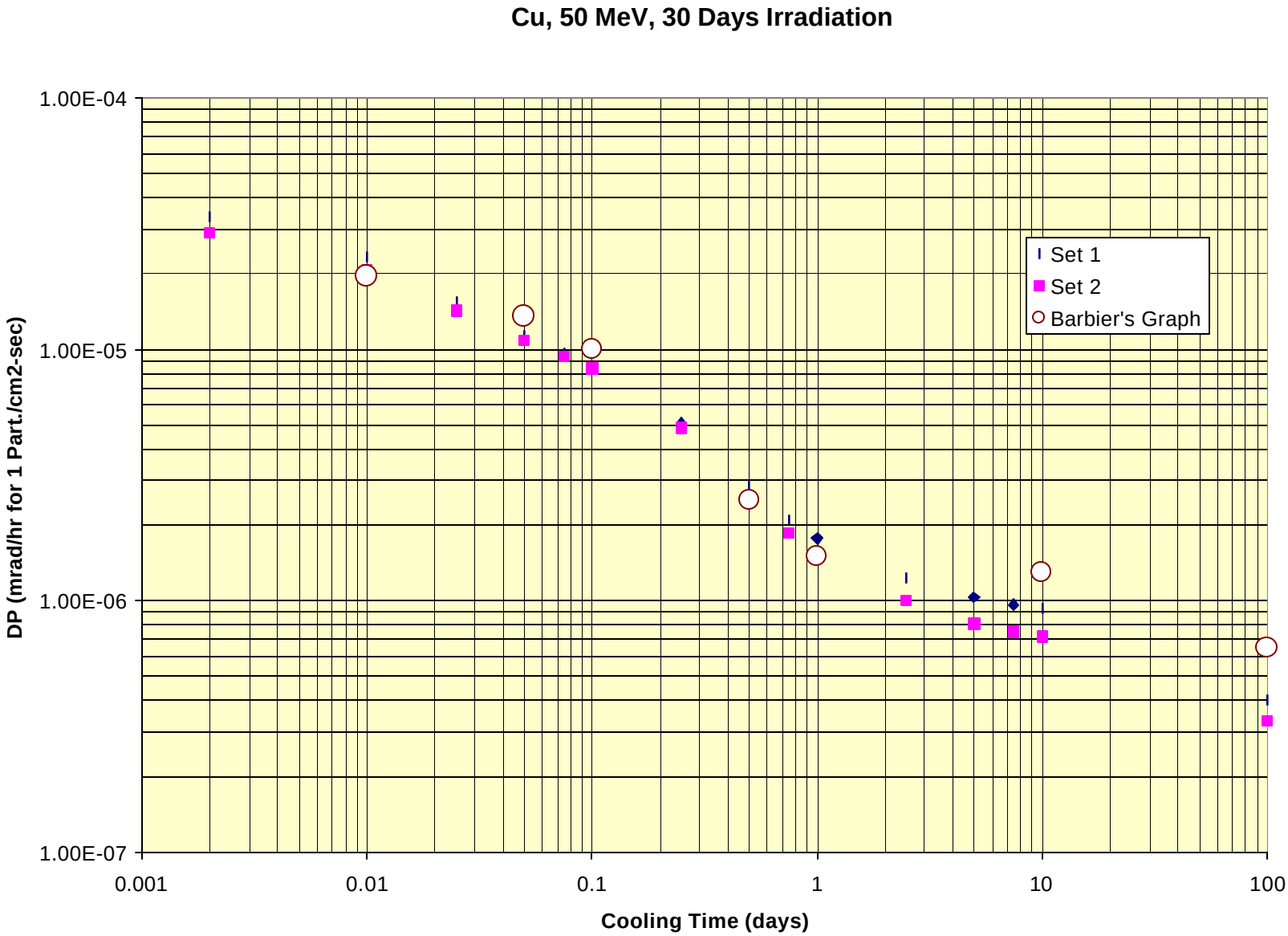

Fig. 14. Danger Parameter for Cu at 50 MeV and 30 Days Irradiation

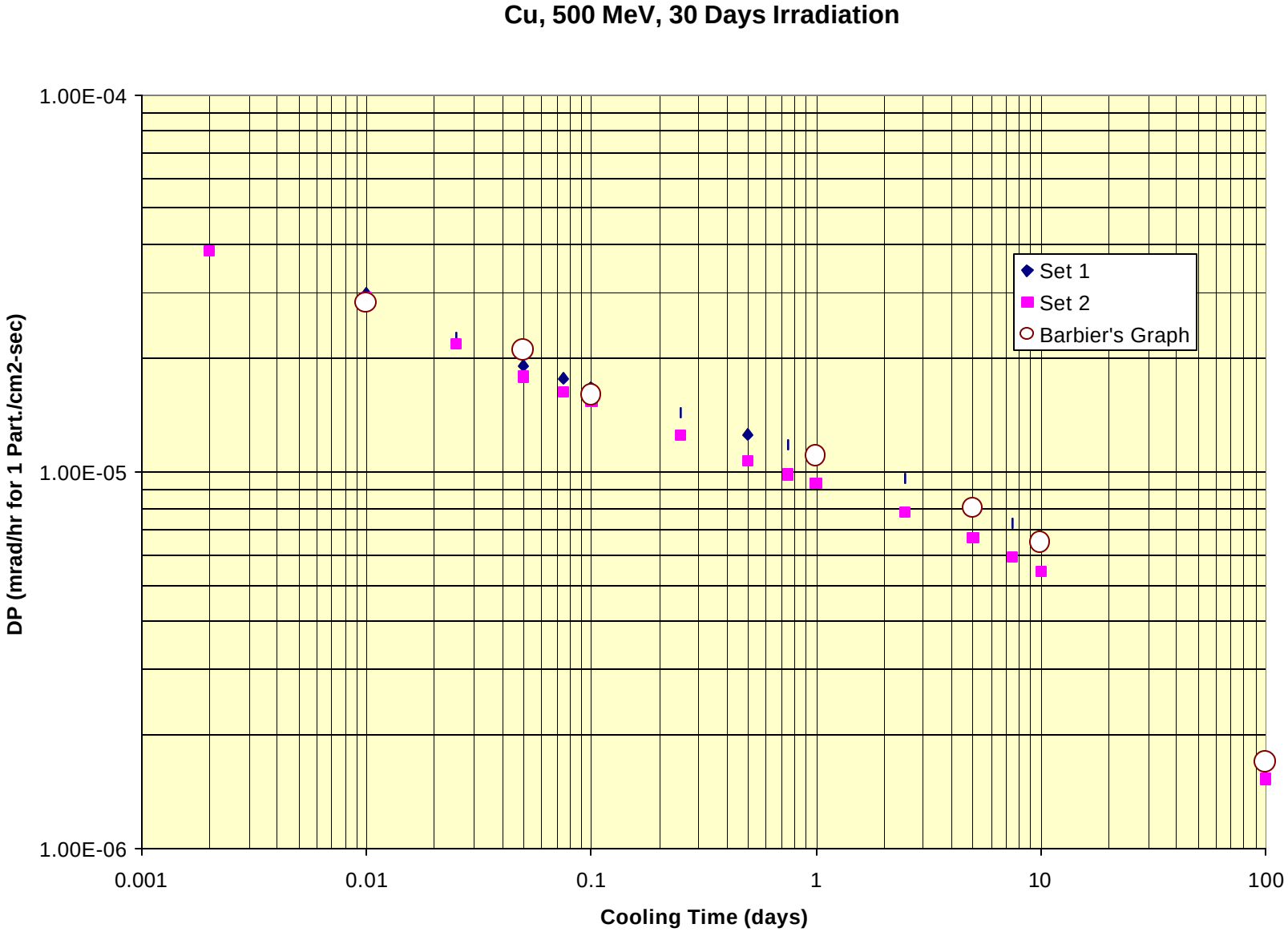

Fig. 15. Danger Parameter for Cu at 500 MeV and 30 Days Irradiation

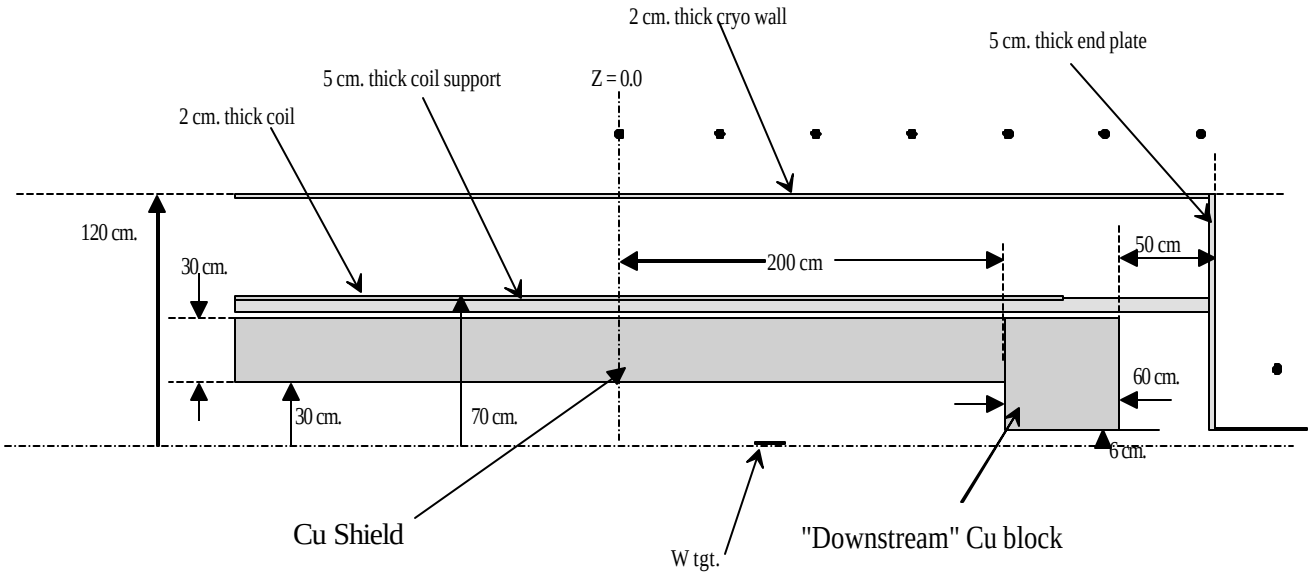

[Dark Circles Indicate Points of Evaluation]

Fig. 16. Approximation of MECO Target Region

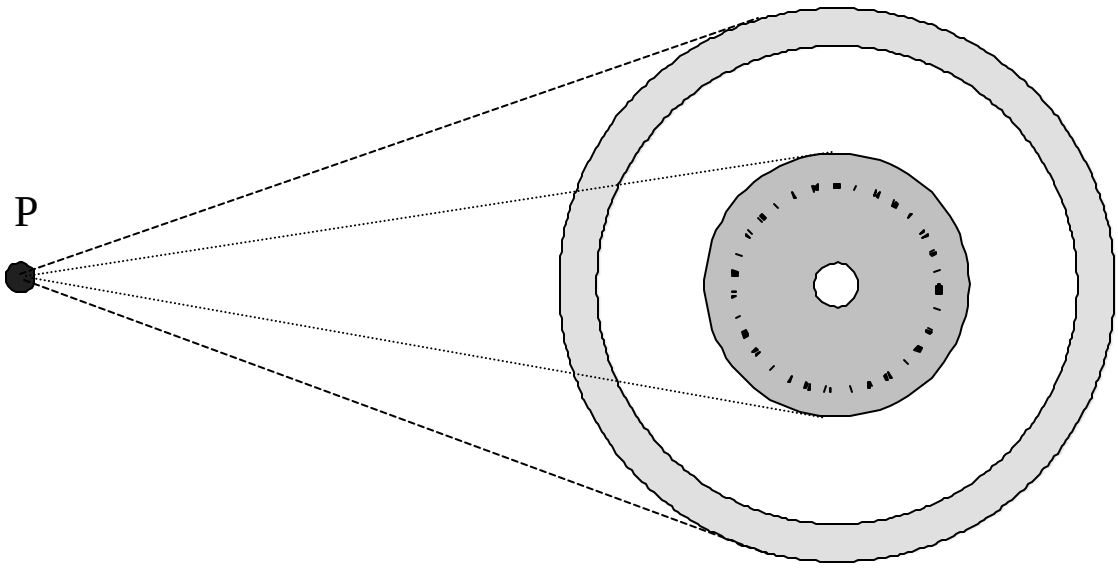

Fig. 17. Highly Schematic “Side View” of the MECO Target Region (see text)

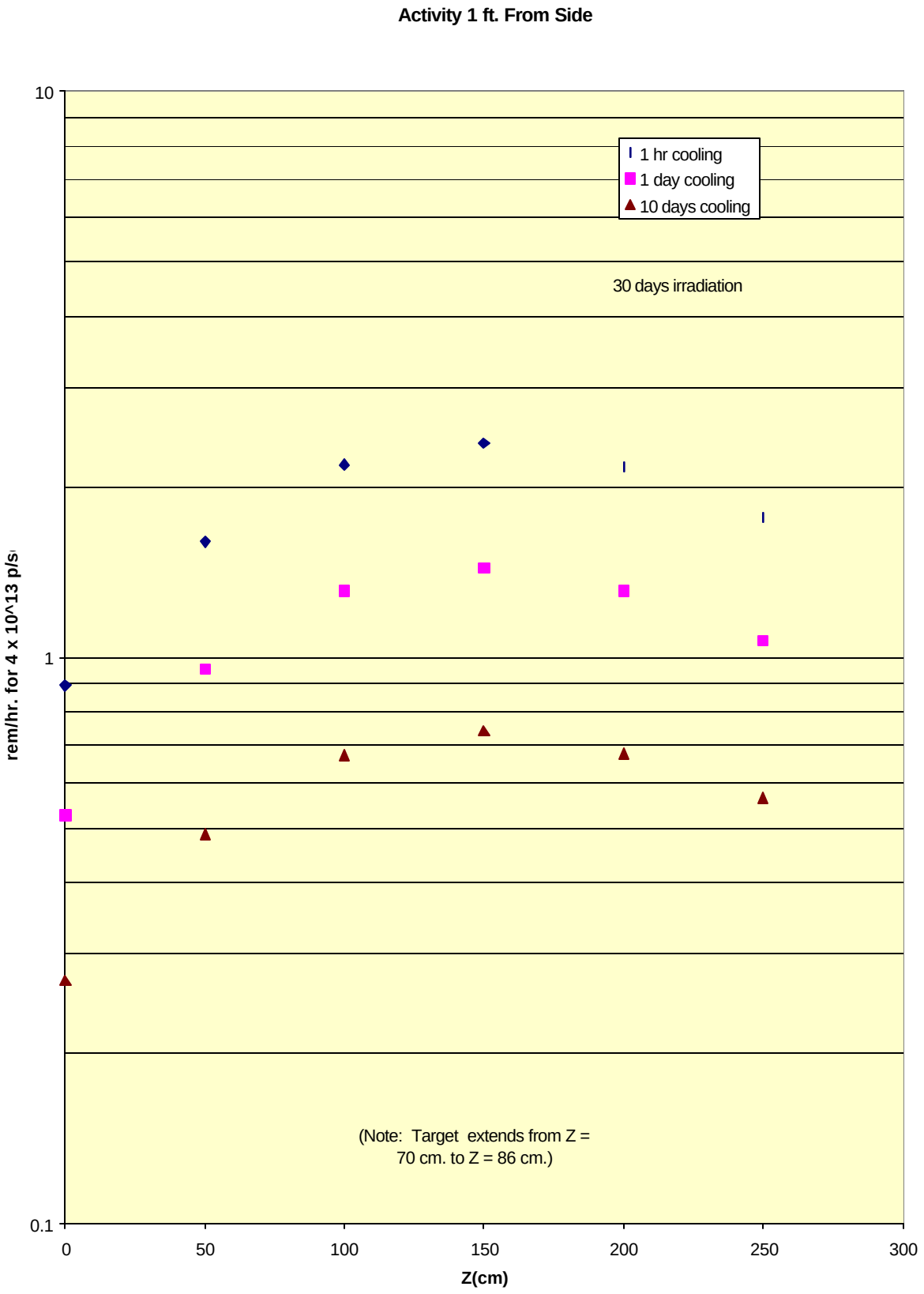

Fig. 18. Estimated Activity for the Points 1 Ft. Outside the Cryo. Wall in Fig. 16

Appendix 1

The following pages show estimated Danger Parameter graphs corresponding to what is called 'Set1' in the text. All photon-emitting nuclides with half life greater than 1 minute have been included.

These graphs differ from those of Barbier chiefly in that cross-sections from MCNPX 2.1.5 have been used in the absence of data for nuclides with atomic weight A_T or A_T-1, and (also in the absence of data) the average of cross-sections given by MCNPX and by the Rudstam formula have been used otherwise. The meaning of "data" is also not entirely clear as discussed in the text.

The calculations were for irradiation times of 1 day, 7 days, 30 days, and 360 days. Cooling times range from .002 days to 100 days although no data points between 10 days and 100 days were included. To enhance clarity in the most useful regions, all the data points are not necessarily shown. As an example, Fig. A1.3 is for SiO_2 at 50 MeV. In order to keep the total range to 4 orders of magnitude, values beyond 5 cooling days for 1 day of irradiation were not shown. Also note that the values below .25 days of cooling for irradiation times of 7, 30, and 360 days are negligibly different, so that only the 7 day irradiation period is plotted.

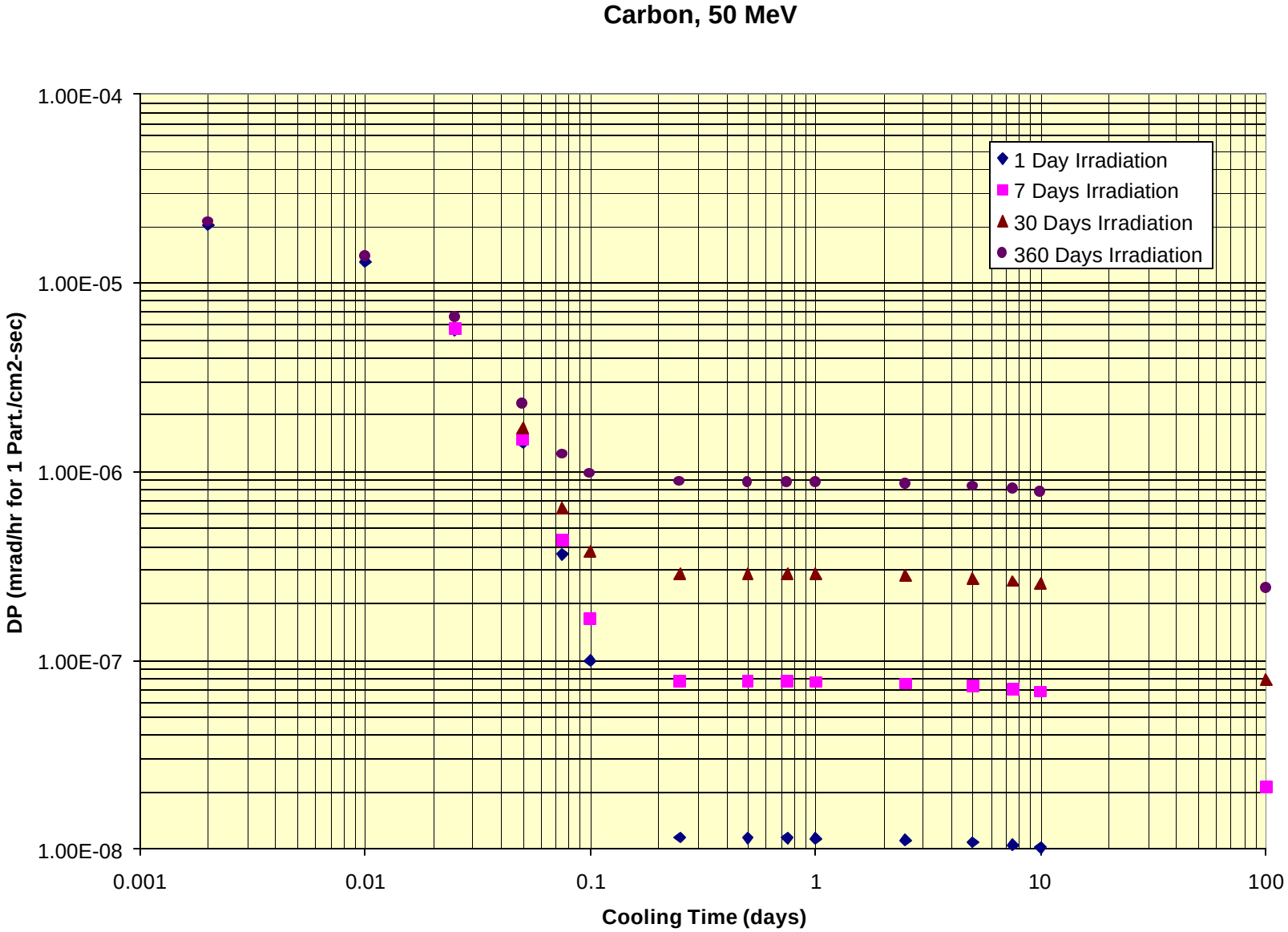

Fig. A1.1 C at 50 MeV

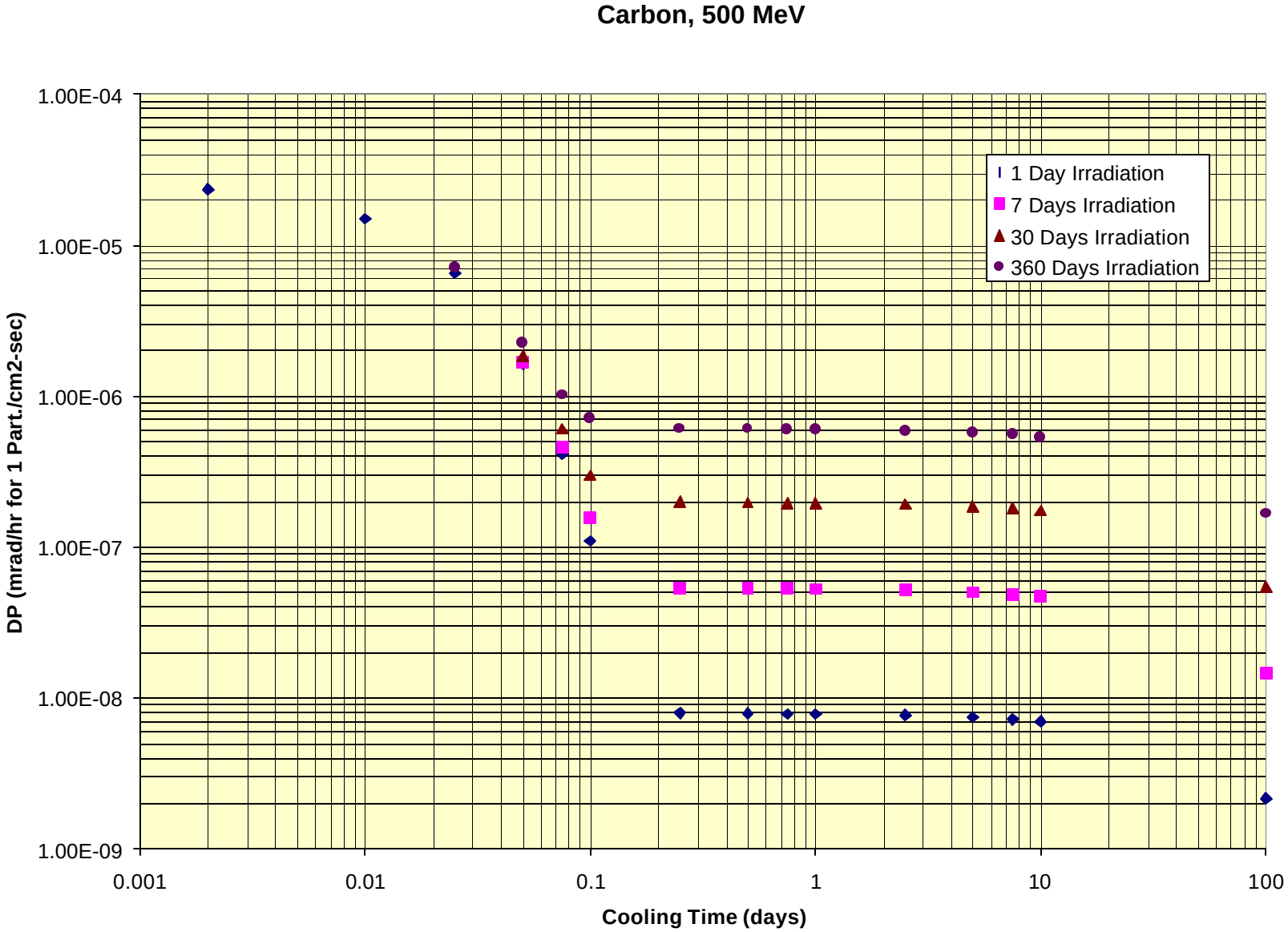

Fig. A1.2 C at 500 MeV

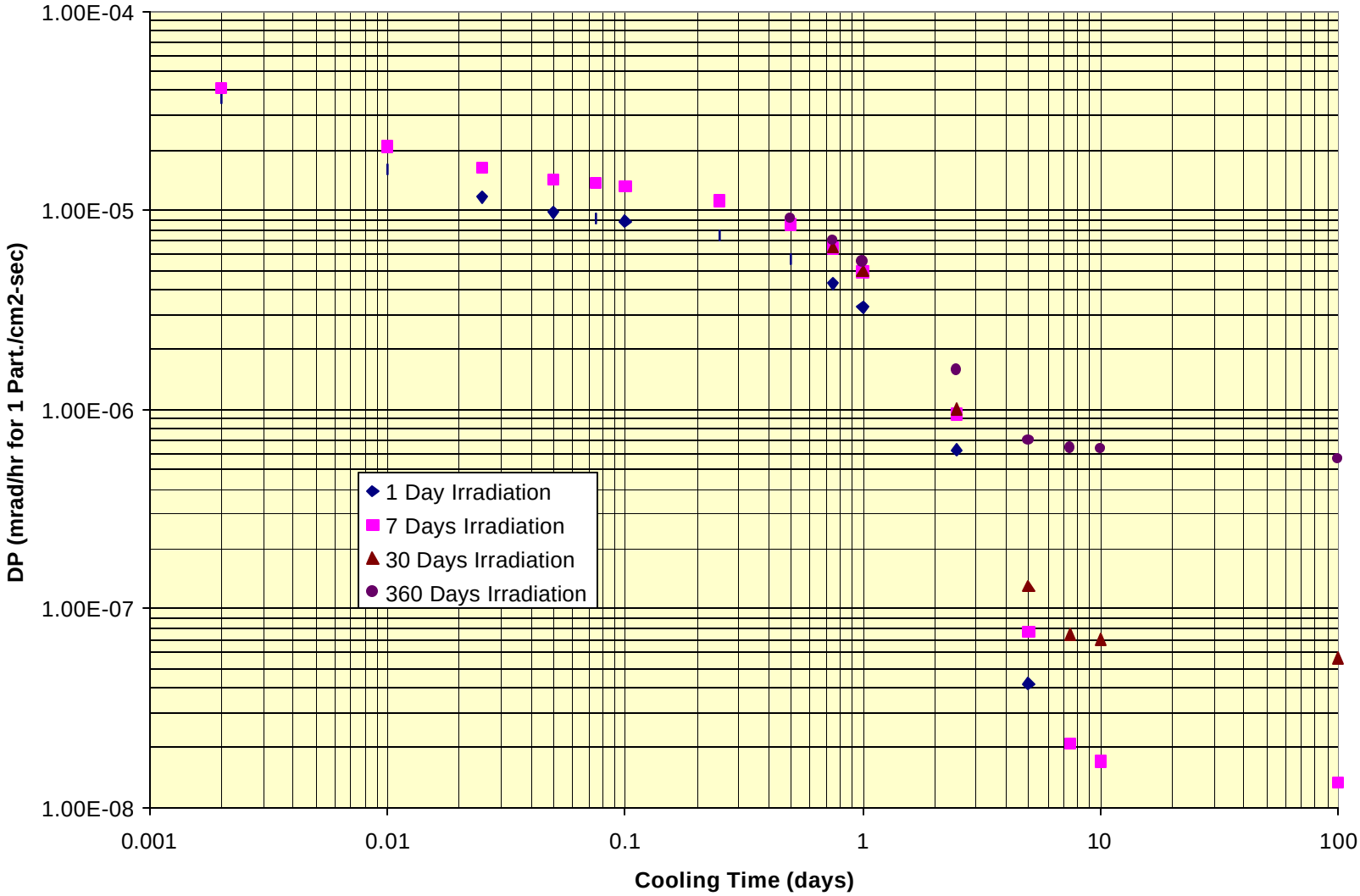

Fig. A1.3 SiO_2 at 50 MeV

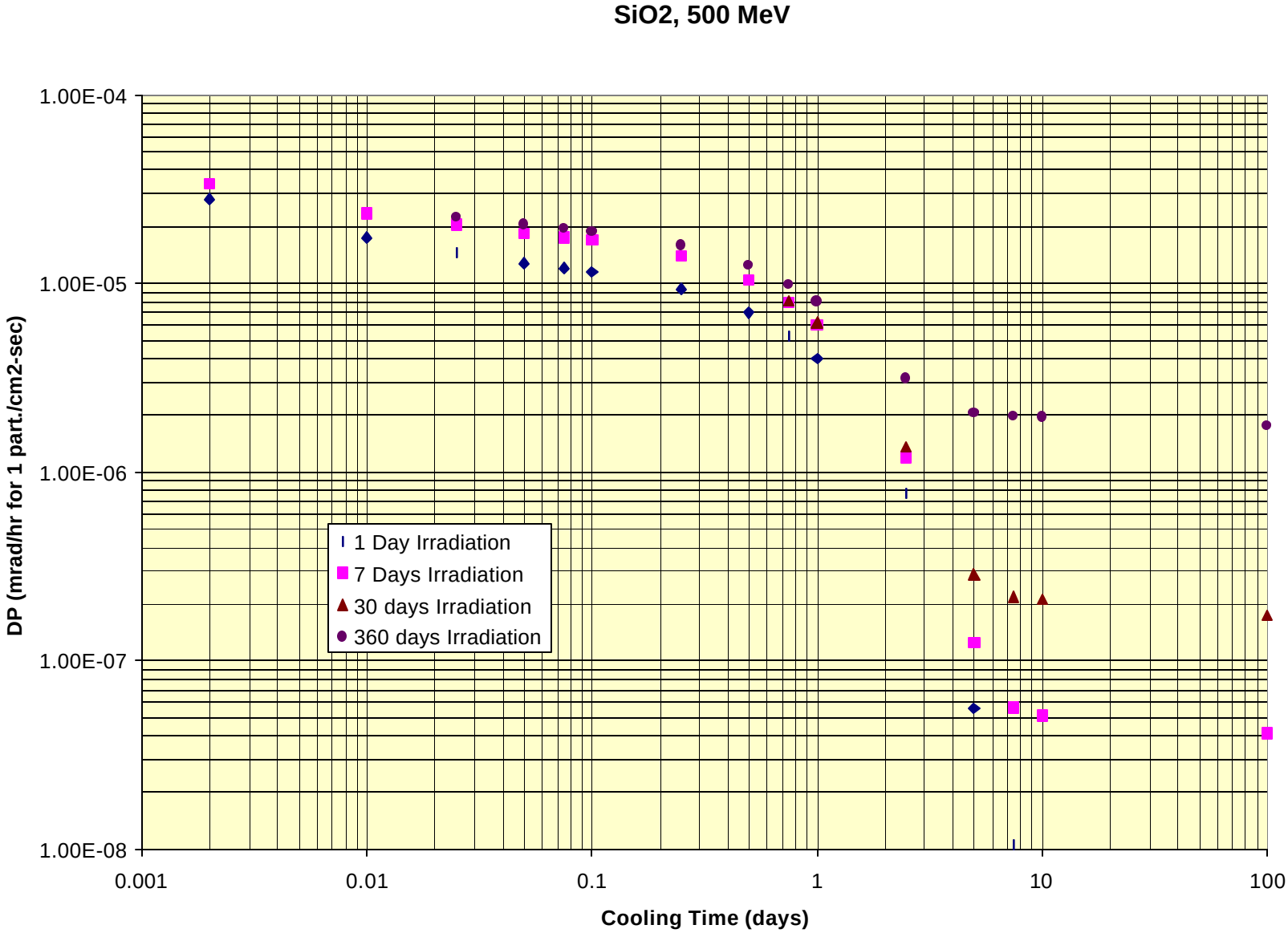

Fig. A1.4 SiO_2 at 500 MeV

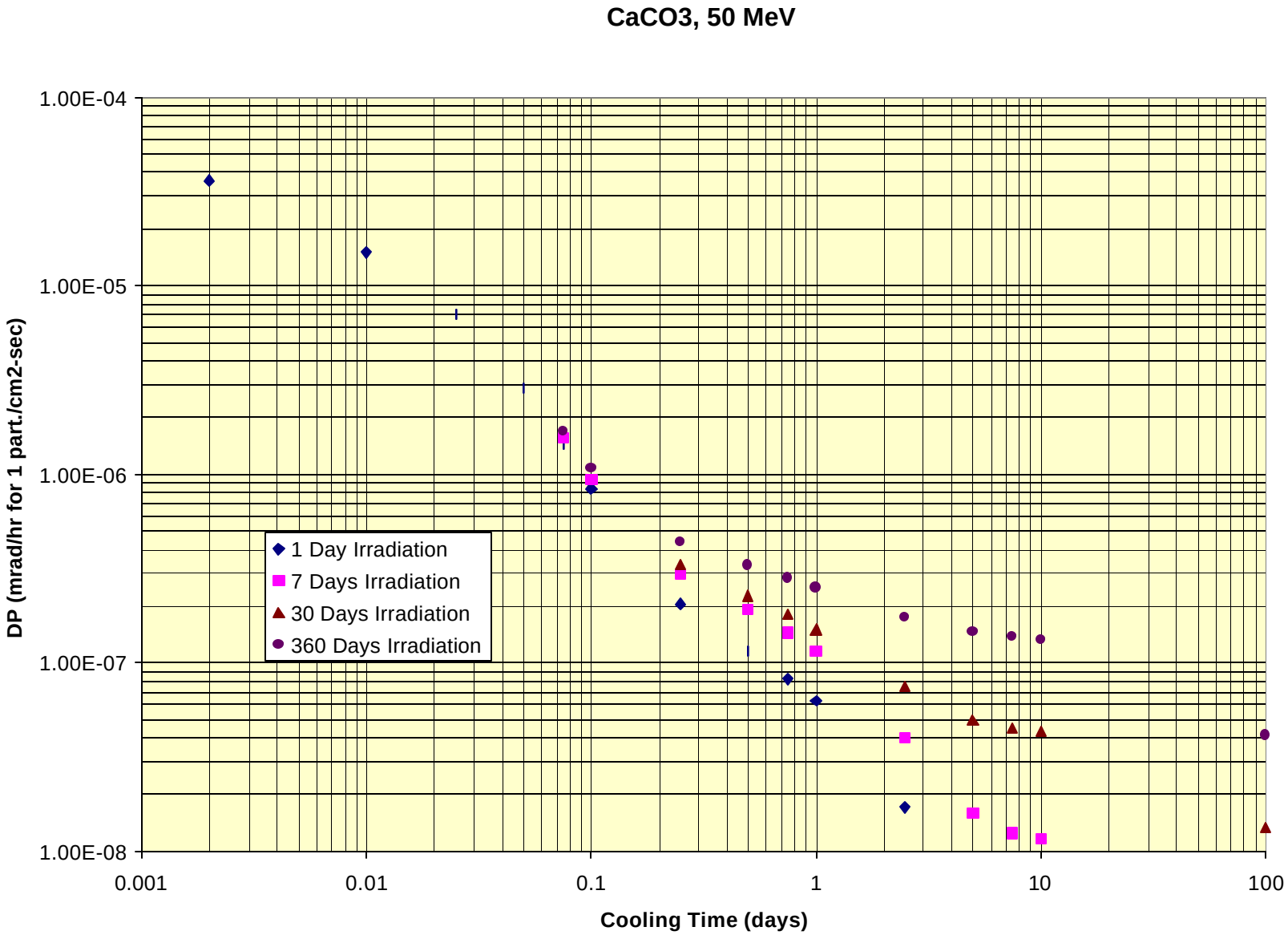

Fig. A1.5 $CaCO_3$ at 50 MeV

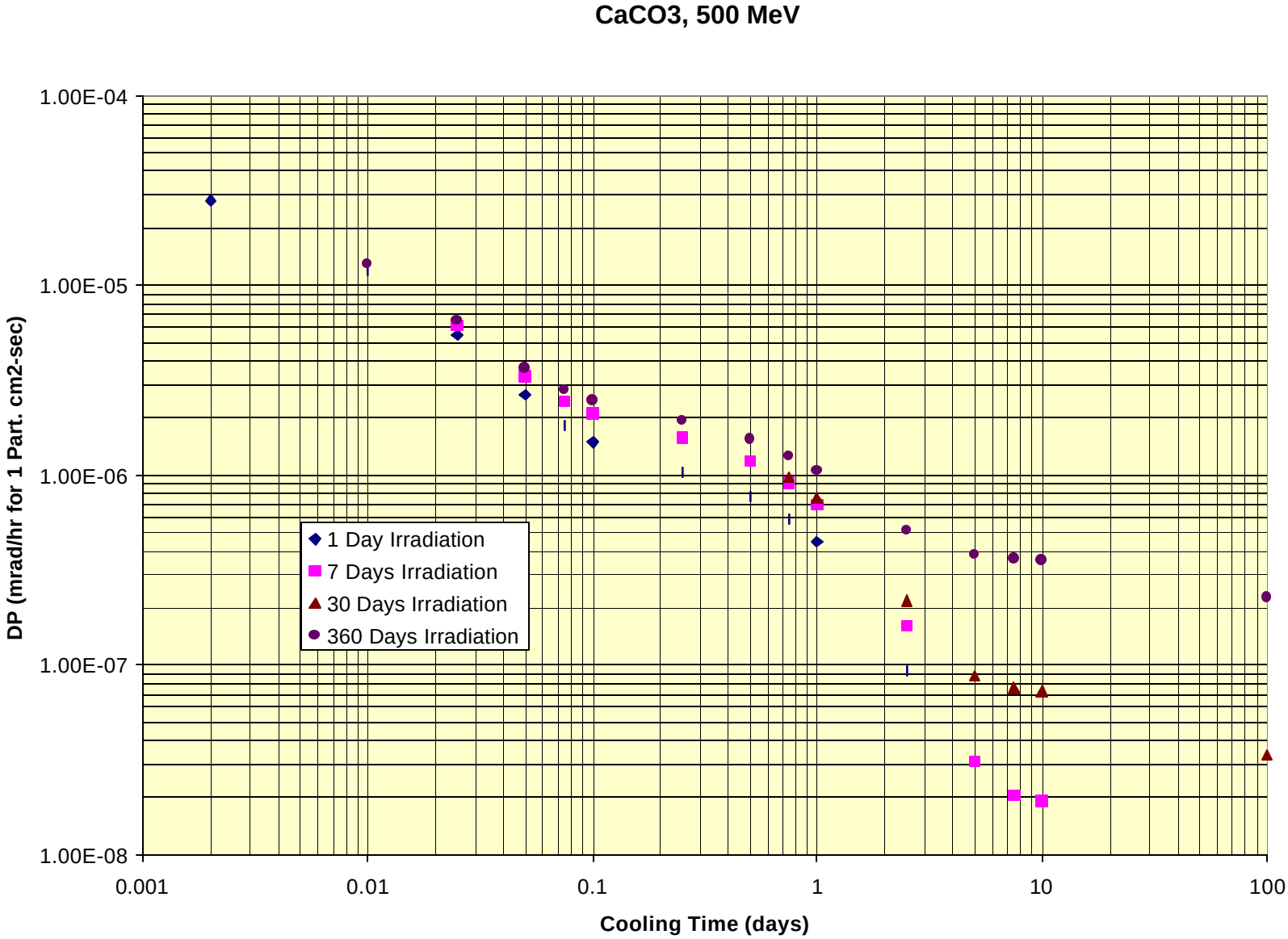

Fig. A1.6 $CaCO_3$ at 500 MeV

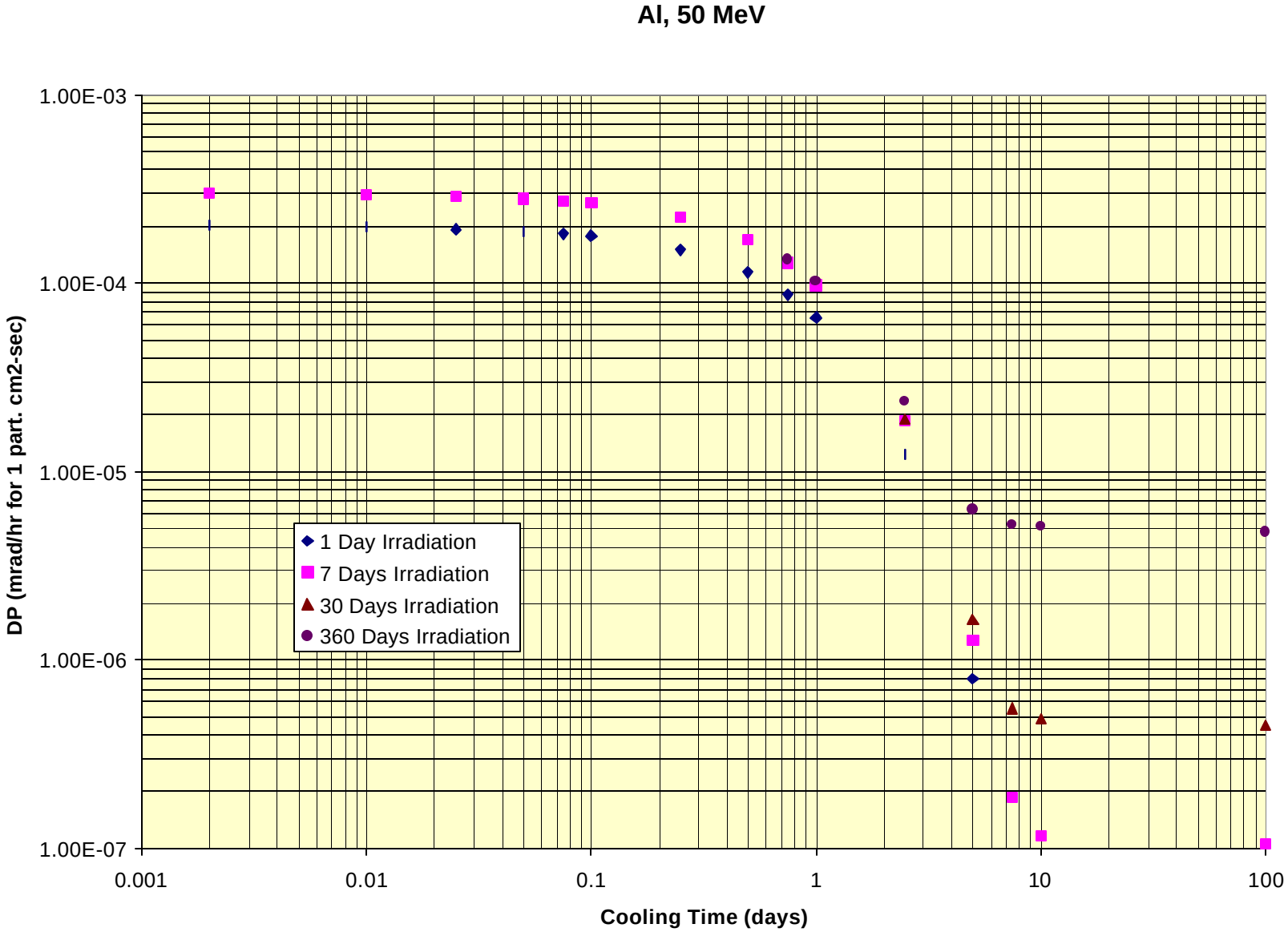

Fig. A1.7 Al at 50 MeV

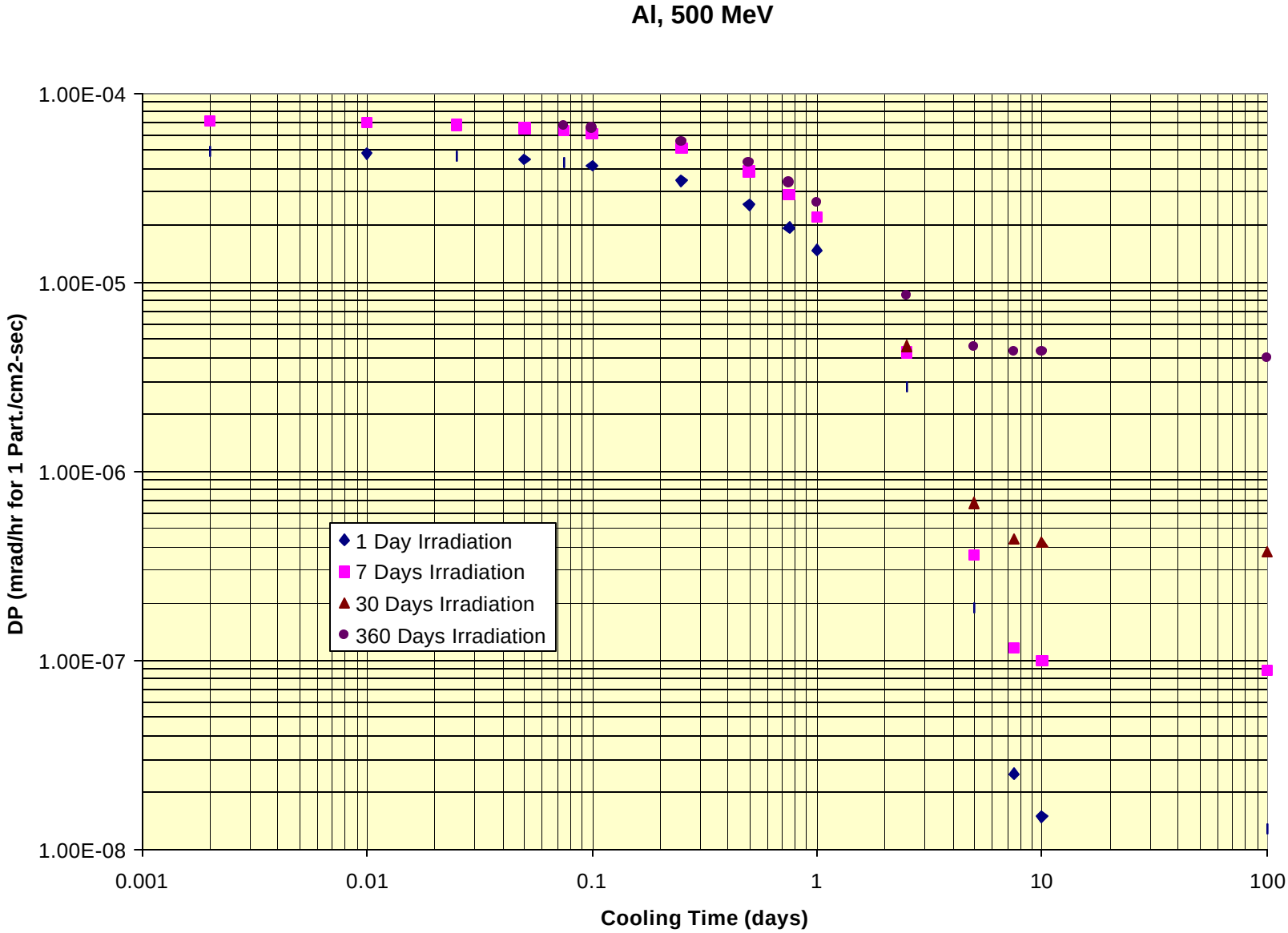

Fig. A1.8 Al at 500 MeV

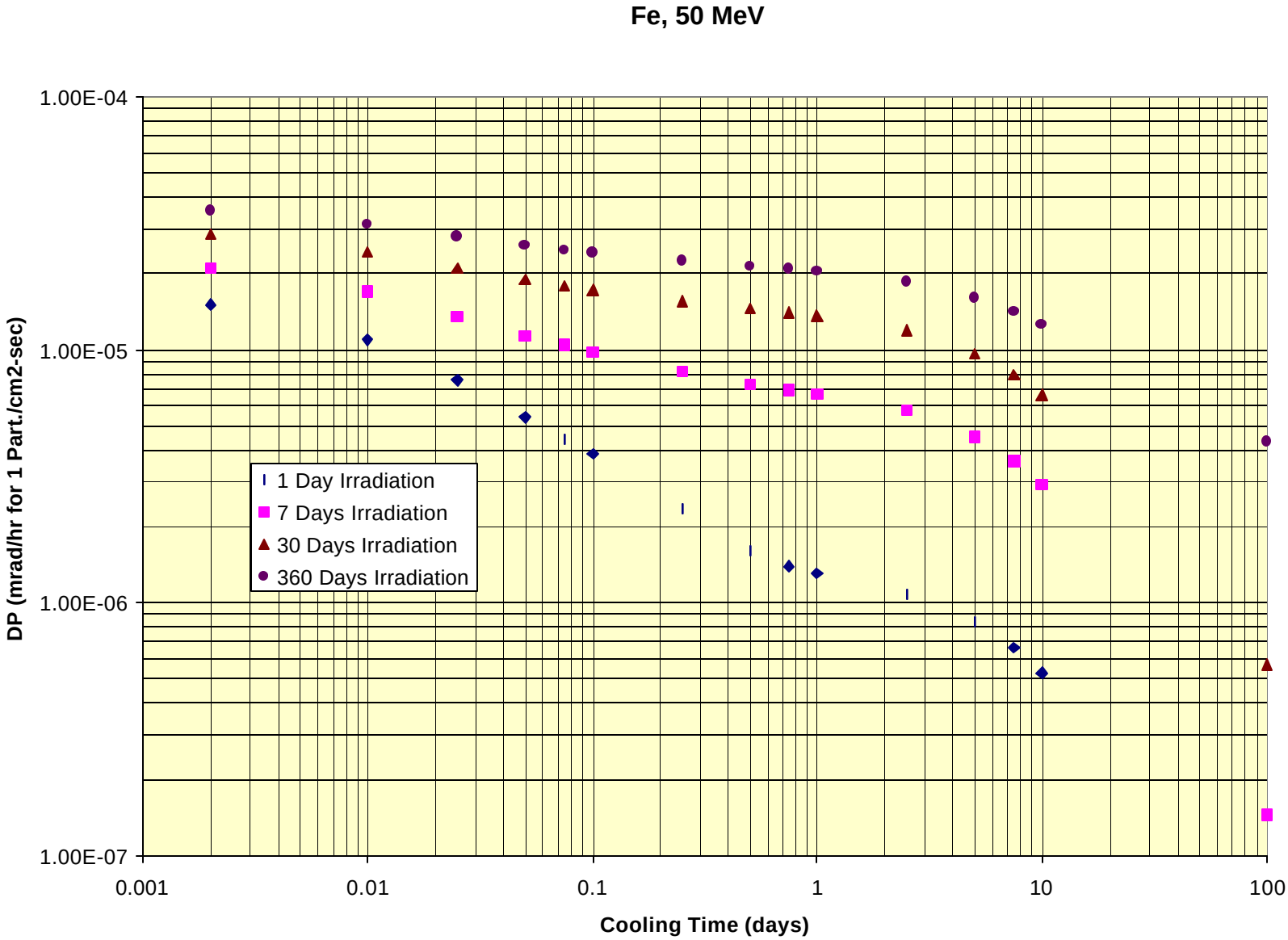

Fig. A1.9 Fe at 50 MeV

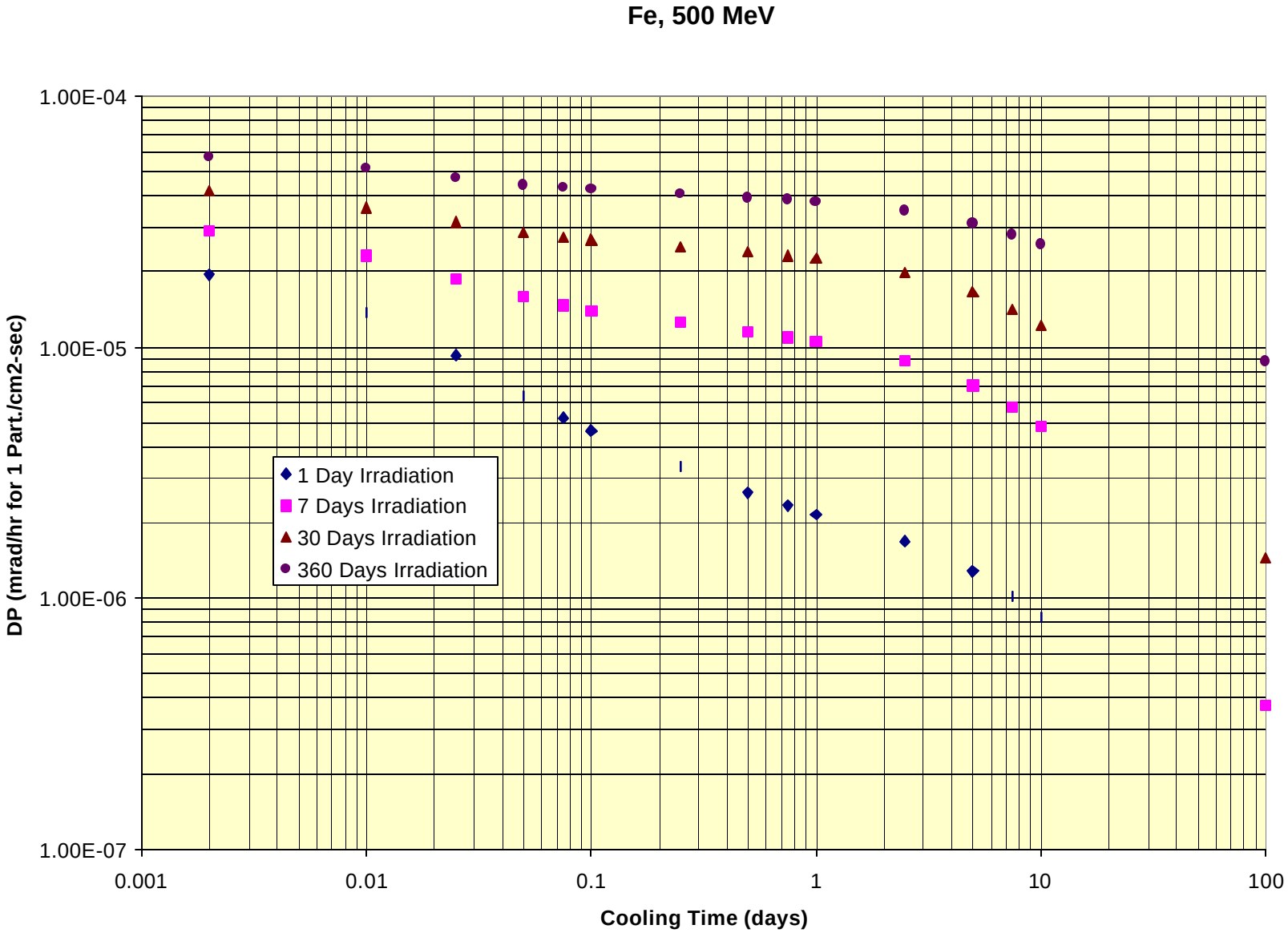

Fig. A1.10 Fe at 500 MeV

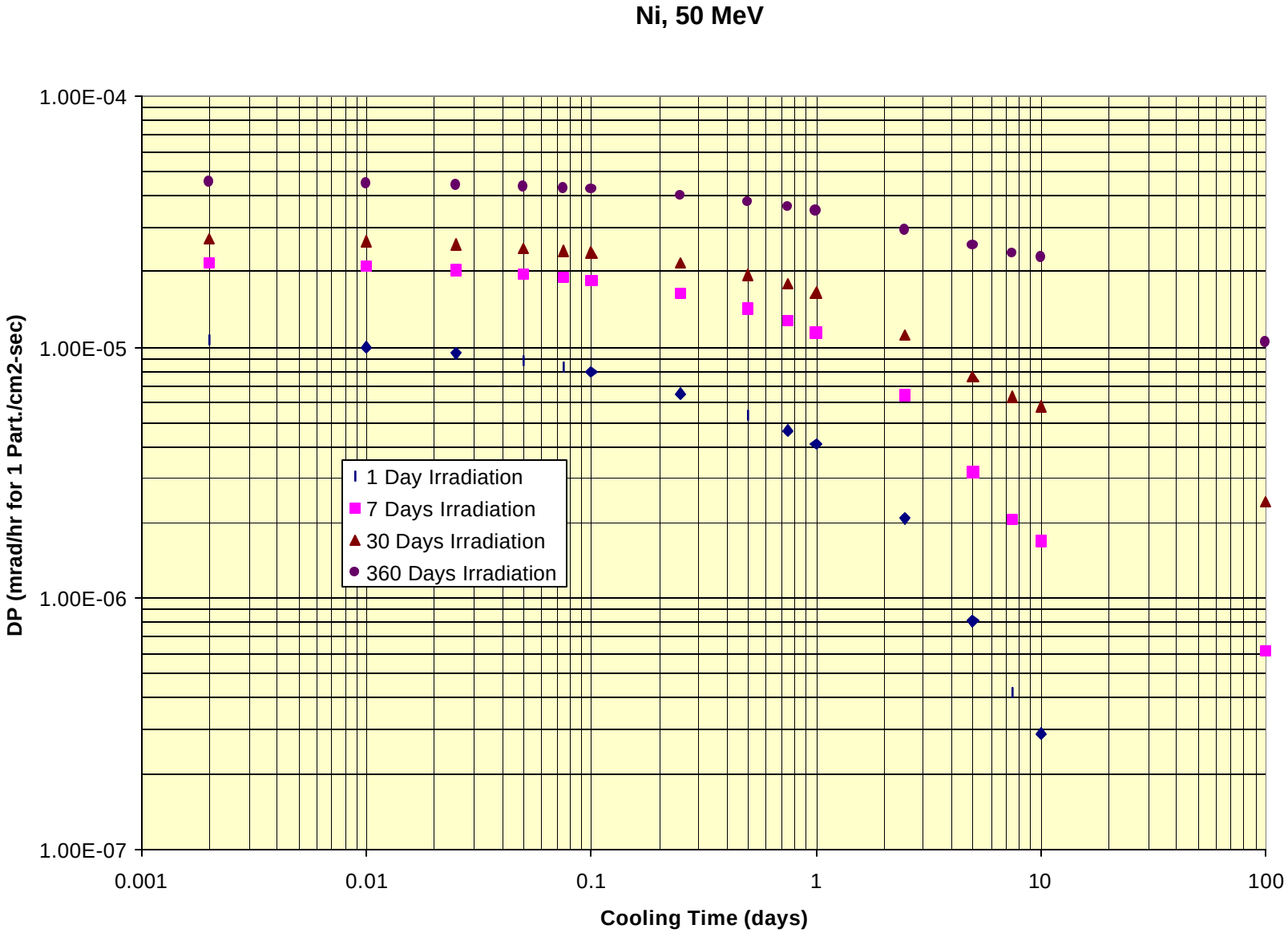

Fig. A1.11 Ni at 50 MeV

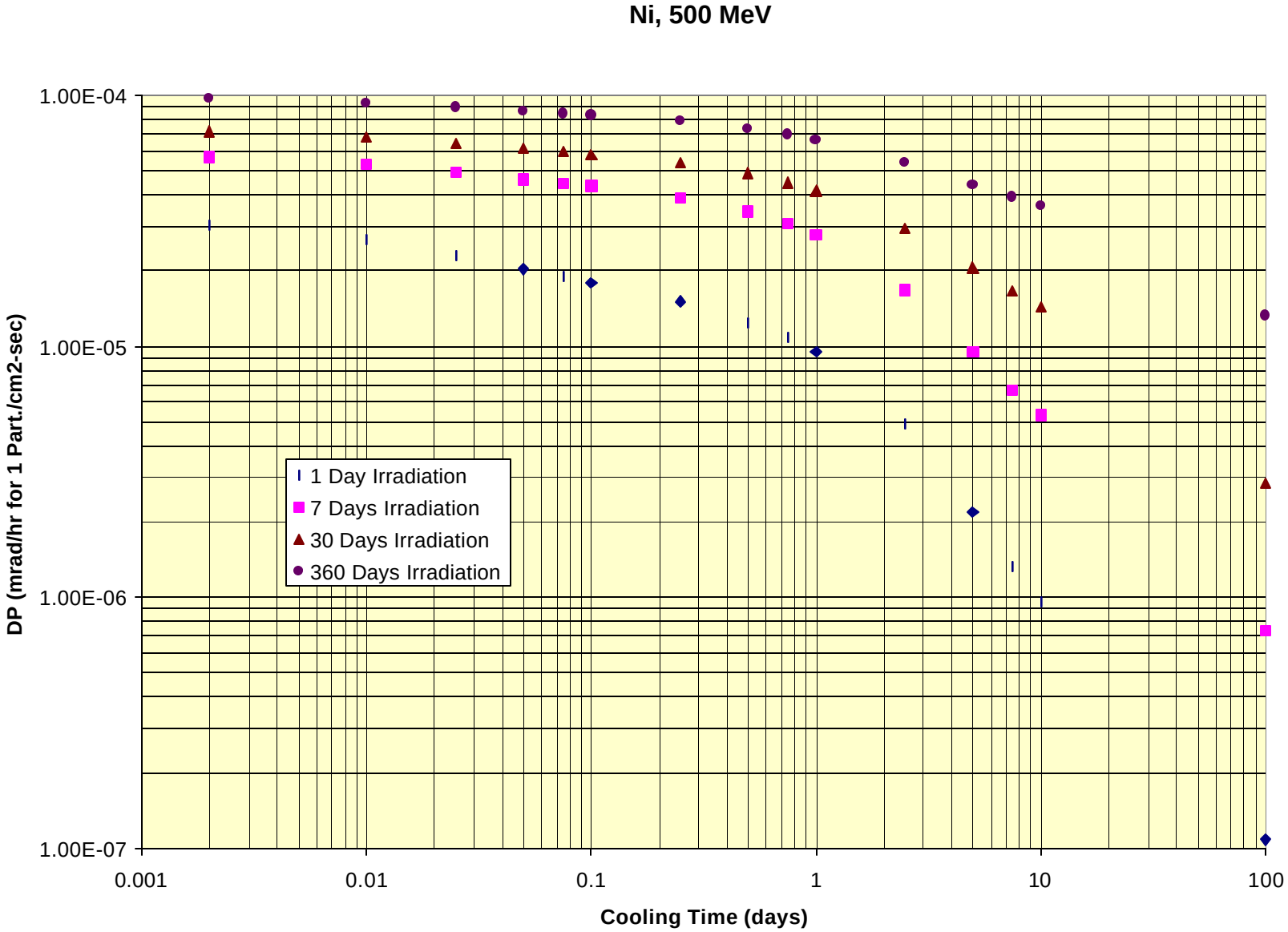

Fig. A1.12 Ni at 500 MeV

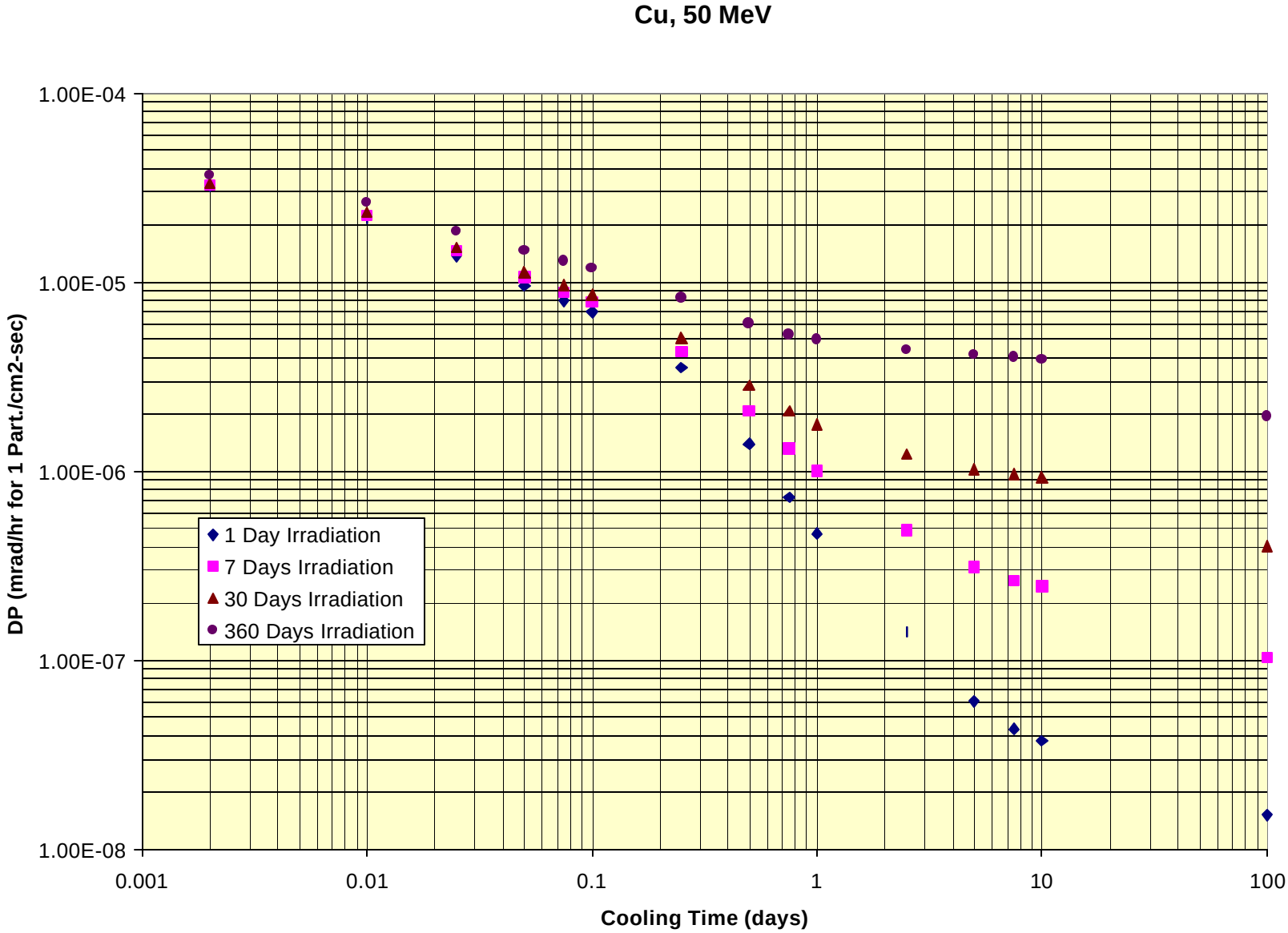

Fig. A1.13 Cu at 50 MeV

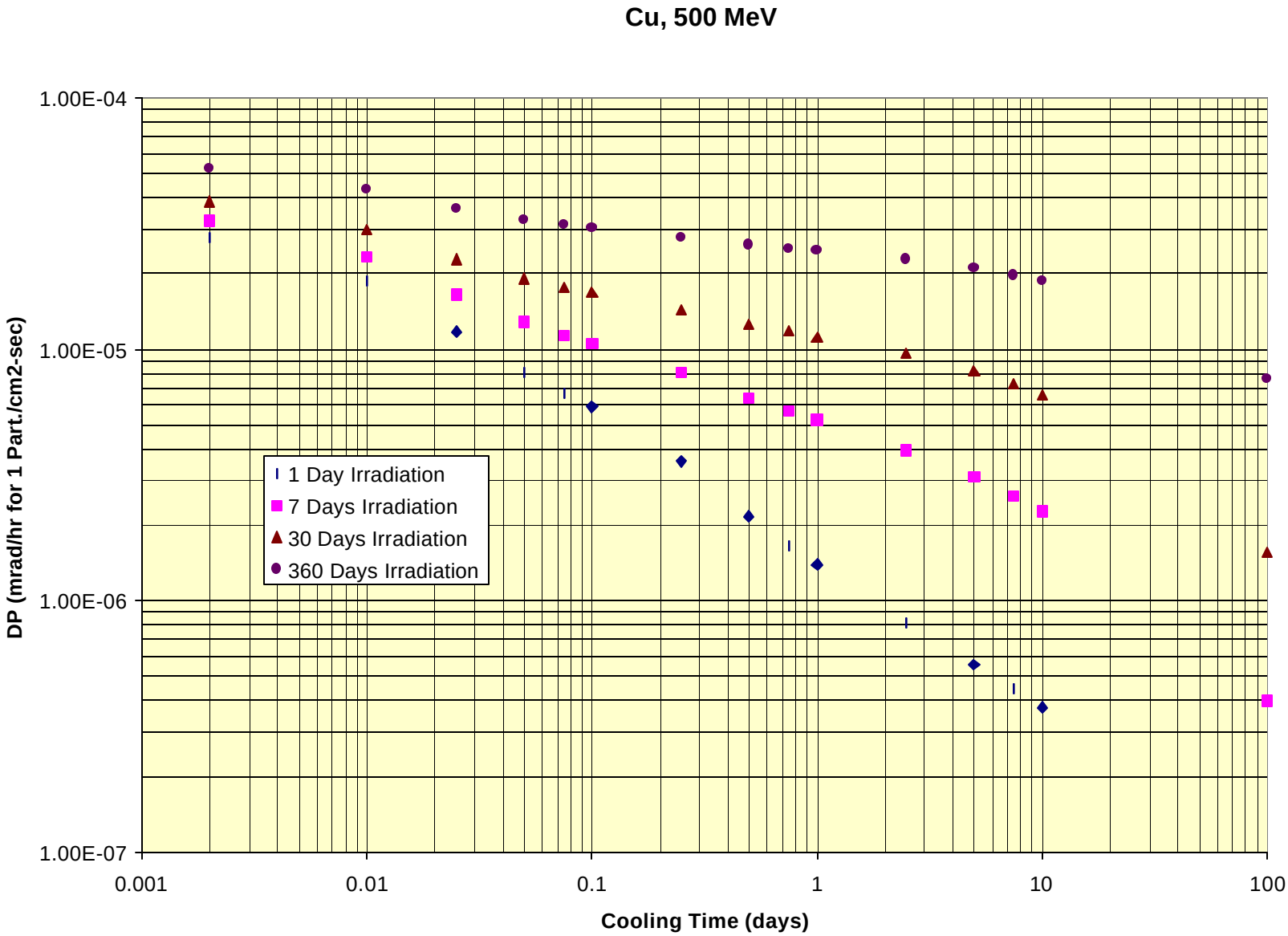

Fig. A1.14 Cu at 500 MeV